VIRGINIA POLYTECHNIC INSTITUTE AND STATE UNIVERSITY

EVALUATION OF PAVEMENT SURFACE FRICTION SEASONAL VARIATIONS

Thesis submitted to the faculty of the Virginia Polytechnic Institute and State University in partial fulfillment of the requirements for the degree of

Master of Science in

Civil and Environmental Engineering

Oscar Daniel Gonzalez Rodriguez

COMMITTEE MEMBERS:

Dr. Gerardo W. Flintsch, Chair

Dr. Edgar de León Izeppi

Dr. Linbing Wang

January 21, 2009. Blacksburg, Virginia, USA

Key Words: Friction, Seasonal Variations, Locked Wheel Trailer, DFtester, Friction Correction Factors.

EVALUATION OF PAVEMENT SURFACE FRICTION SEASONAL VARIATIONS

Oscar Daniel Gonzalez Rodriguez

ABSTRACT

Wet-pavement friction is one of the most important pavement characteristics in relation to highway safety. This property is difficult to measure because it is affected by many vehicle, driver, pavement, and environmental parameters. In particular, it has been observed that both short- and long-term seasonal variations impact wet-pavement friction. Temperature, rainfall, and contaminants accumulated on the pavement surface affect the friction measurements.

The objective of this thesis was to quantify the effect of seasonal variations on pavement surface friction measurements on hot-mix asphalt surfaces. Monthly measurements of friction and texture were collected on nine hot-mix asphalt sections at the Virginia Smart Road for a year and a half. Friction was measured using two locked-wheel trailers and a Dynamic Friction Tester. Measurements with the two types of equipment were conducted in the same day. Macrotexture measurements were taken using a Circular Texture Meter on the same locations used for the DFTester measurements.

In order to compare friction measurements on the different surfaces, the monthly friction values were normalized by dividing the value obtained each month by the August 2007 measurements, which were theoretically the lowest friction numbers. The resulting ratios were considered friction correction factors to bring the friction measurements to the lowest value. After studying the friction variation throughout the year, sinusoidal models were fitted to the data to predict monthly correction factors for measurements at different speeds using both devices.

The main conclusion of this investigation is that seasonal variation has a significant effect on pavement friction measurements. The general trend observed is that the measurements are higher in the winter months than in the summer months. This tendency follows a cyclical sinusoidal pattern throughout the year, similar to the air temperature variations. This suggested that temperature was at least one of the factors that affected the fiction correction factors. Better coefficients of determination were obtained for the DFTester models than for those for the locked-wheel devices. However, the sinusoidal model determined for the locked-wheel device at 64 kph (40 mph), which is the standard test velocity, fit relatively well the measured friction correction factors. Average friction correction factors for the Commonwealth of Virginia were proposed using these models.

The study also showed that the friction correction factors are speed-dependent and are affected by the macrotexture of the pavement surface. The maximum (winter) friction correction factors were found to decrease with increased macrotexture for both devices at all speeds. The effect is more pronounced, however, for the locked-wheel measurements than for the DFTester measurements.

ACKNOWLEDGEMENTS

First, I would like to thank God for giving me the opportunity to complete my dream of studying at Virginia Tech, full of well recognized and dedicated professors and good classmates. I would like to express my greatest gratitude to Dr. Gerardo Flintsch; who was a good mentor, a great example of what an excellent professor and person is, but most importantly, a good friend who had always a good advice to give. Thank you for all your unconditional support, patience, hours of work, and committed dedication to your students. Thank you for giving me the privilege to work with you. I would also like to extend all of my gratitude to Dr. Linbing Wang and Dr. Edgar de Leon Izeppi. Thank you for being part of this excellent committee which was always willing to help and support.

I would like to thank my teachers of life; my parents, Oscar G. and Laura Elisa, for all their never-ending hours of thinking of me, for their support and their good example in life. Thank you mom and dad for giving me always hope and believe in me. I wouldn't reach this goal if it wasn't for you. Thank you, to my sister and brother, Laura and Cesar, for encouraging me and supporting me through all my life. Thank you to my Grandmother, Elva Elisa who was part of this dream, I am sure, and somewhat in heaven you are happy about this accomplishment.

Thank you, to Billy Hobbs, to all the people from VDOT and Kevin McGhee from the Virginia Transportation Research Council who were always kind and enthusiastic about this investigation.

Last but not least, I thank all my friends in Blacksburg and Mexico for making this possible, Daniel, Orlando, Fernando, Julio, Luis, Mario, Soly, Becky, Nestor, Sebastian, Jean Paul, Ricky, Genaro.

Thank you to my country, Mexico for giving me a great culture and education. Thanks, to this country USA for giving opportunities and high-level education to international students around the world.

Con Todo mi Corazón, Gracias. El que persevera, alcanza

Oscar Daniel González Rodríguez

TABLE OF CONTENTS

LIST OF FIGURES

The author of Figure 10. SN_0 and PNG versus Pavement Temperature (Luo and Flintsch, 2004), gives permission to use this figure for this Thesis. Unless noted, all the other images are property of the author.

LIST OF TABLES

CHAPTER 1. INTRODUCTION

1.1 Background

One important contributing factor to automobile crashes is slippery pavements. Although conditions such as road geometry, traffic flow, and road conditions are also influential, it has been estimated that 35 percent of crashes are caused at least partially by skidding (NCHRP, 1992). The Maryland State Highway Administration's Traffic and Safety Analysis Division reports that approximately 18 percent of fatal crashes and 24.3 percent of all crashes occur when pavements are wet (MDSHA, 2002). Wet pavement friction is one of the factors that determine highway safety. For pavement monitoring in the United States, friction is defined as "the retarding force generated by the interaction between a pavement and a tire under locked non-rotating conditions" (ASTM E-17). Numerous studies worldwide have shown a direct relationship between crash risk and friction coefficients measured on roads. This association has led to a common conclusion: crash risk decreases with increasing friction (AUSTROADS, 2004).

The main propose of measuring and monitoring tire-pavement friction is to reduce the number of crashes and fatalities due to skidding. According to Kennedy, Young, and Butler (1990) an improvement of 10 percent in the average level of skid resistance could result in a 13 percent reduction in the wet-skid crash rate. Thus, friction should be monitored as part of the pavement management process. However, this property of the pavement surface is affected by temperature, rainfall, and other environmental factors, as well as vehicle and tire characteristics. An enhanced understanding of the change in pavement friction properties due to environmental conditions (i.e., temperature, precipitation, and aging) may help agencies make better pavement management decisions.

Hall et al. (2006) classified the variables that affect tire-pavement friction into the following categories: (1) pavement surface characteristics (i.e., microtexture and macrotexture), (2) traffic variables (e.g., slip speed), (3) tire properties (i.e., foot print and inflation pressure), and (4) environment (i.e., climate, wind, temperature, precipitation, and contaminants). In particular, environmental (climatic) factors can have both short-term and long-term effects. For example, since the tire rubber and some pavement materials (hot-mix asphalt) are viscoelastic, temperature should affect their properties. Although many researchers have studied how tire-pavement friction is affected by temperature and other environmental factors, this phenomenon is still not well understood.

For many years, researchers and practitioners have observed seasonal variations of pavement friction measurements. These measurements experience variations due to traffic and weather-related

factors. Traffic affects friction by polishing the aggregate; its effect is cumulative over time. On the other hand, weather-related factors such as dry days before the test, air temperature, wind, and precipitation are partially responsible for short-term and long-term variations on surface friction properties. For example, studies in the United States (Hill and Henry, 1978), New Zealand (Wilson, 2006), and the United Kingdom (Croney and Croney, 1998) have shown that friction properties of pavement surface vary significantly within relatively short periods of time. Furthermore, these variations follow an approximate sinusoidal fluctuation pattern due to seasonal change (Jayawickrama and Thomas, 1998). This resembles the temperature variations throughout the year. However, some researchers have pointed out that seasonal variation cannot be considered a decisive indication of the dependence of pavement friction on temperature. For example, Cenek et al. (1999) indicated that skid resistance variation in the United Kingdom is due mostly to precipitation effects. This effect is explained by less precipitation and greater evaporation rates during spring and early summer, which lessens the removal of lubricating agents and other contaminants on the road surface by rainwater.

1.2 Problem Statement

Friction is a very important road safety factor. However, this property is difficult to monitor because its measurement is affected by many factors. These include road geometry, traffic characteristics, weather condition (such as snow, rain, or ice), vehicle speed, construction quality, and type of tire, among others. In particular, it has been observed that seasonal factors such as temperature, precipitation, and dry days before the test affect tire-pavement friction measurements. Although several researchers have attempted to explain the effects of seasonal variation on pavement surface friction properties, there is not general agreement on the magnitude of the effect. In particular, disagreement still exists about the impact of temperature on tire-pavement friction. Some researchers have documented that skid resistance is affected by seasonal variations. For example, Giles et al. (1964) observed a significant effect of air temperature on the measured friction properties. Bazlamit and Reza (2005) reported a general trend of lower friction during warm seasons than in colder seasons. However, other studies have reported negligible effects (Mitchell et al. 1986). The discrepancies may be partially explained by the use of different measuring equipment. Therefore, it is important to conduct more studies under controlled conditions to gain a better understanding of seasonal effects on pavement surface friction properties.

1.3. Objective

The main objective of the thesis is to quantify the effects of seasonal variations on the measurement of the friction and macrotexture properties of hot mix asphalt (HMA) surfaces and, if required, to develop monthly friction correction factors to adjust friction measurements.

1.4 Significance

The investigation of friction seasonal variations on pavement surfaces is a worldwide concern. Researchers and practitioners have pointed out that measurement of friction on the same pavement surface sections experiment variations throughout the year. In order to evaluate these variations, it is necessary to conduct friction measurements on the same pavement surface sections periodically, for example monthly. If significant variations are observed, it is important to adjust the friction measurements by using seasonal or monthly correction factors. This may help agencies around the world make better pavement friction management decisions, and it may help prevent skidding-related crashes.

1.5 Thesis Overview

This research utilized the Virginia Smart Road facility at the Virginia Tech Transportation Institute, which includes HMA and Portland Concrete Cement (PCC) surfaces. Pavement surface properties were collected every month from December 2006 through July 2008. Friction measurements were taken using two locked-wheel trailers and a DFTester. Macrotexture measurements were obtained using a CTMeter. The investigation evaluated friction variation on nine of the HMA sections at the Virginia Smart Road. Monthly friction correction factors were calculated for measurements obtained with the locked-wheel trailers and the DFTester. Sinusoidal models were fitted to the average experimental monthly friction correction factors for various speeds. Furthermore, the effect of macrotexture on the friction seasonal variation was investigated.

This thesis consists of six chapters. Chapter 1 introduces the research objective and provides an overview of the thesis. Chapter 2 contains a review of literature related to friction and texture measurement devices, fundamental friction theories and models, pavement surface characteristics, and factors affecting friction such as temperature and precipitation. Chapter 3 describes the experimental program conducted for this investigation and discusses the pavement sections evaluated, the friction and texture measurement equipment utilized, and the temperature data collected. Chapter 4 summarizes the data collected. Chapter 5 explains the analysis performed and presents the main results of this analysis. Chapter 6 summarizes the main findings and conclusions of the research effort and proposes recommendations for future research.

CHAPTER 2. LITERATURE REVIEW

This chapter critically reviews the main literature related to pavement friction measurements and the effect of seasonal factors on pavement surface properties. Basic concepts, measuring devices, testing standards, and friction models are discussed.

Friction surface properties play an important role in highway safety. According to the National Highway Transportation Safety Administration (NHTSA, 2004), between 1990 and 2003 an average of 6.4 million crashes occurred annually on the nation's highways, resulting in 3 million injuries and 42,000 fatalities per year. This equals a rate of 115 deaths per day. In addition to the loss of human lives, the costs of damaged property, traffic delays, and operations are very high. In 2000, the total cost of crashes was estimated approximately at $230.6 billion (NHTSA, 2004). These crashes occur because of a combination of different factors, falling primarily under the following three categories: (1) driver-related, (2) vehicle-related, and (3) highway-conditions-related (Noyce and Bahia, 2005). Of all these categories, only highway-conditions-related factors can be controlled by highway agencies through better highway designs, adequate pavement friction levels, construction, and maintenance.

2.1 Friction and Texture Measuring Devices

Tire-pavement friction is measured using different devices, including laboratory and field equipment. The laboratory friction testing equipment includes the British Pendulum Tester and the Dynamic Friction Tester (DFTester). These devices can also be used in the field for static measurements. Field friction measuring equipment includes locked-wheel, side-force, fixed-slip, and variable-slip testers. The different devices simulate different operational scenarios. The locked-wheel trailer reproduces emergency braking conditions without anti-lock brakes. The fixed- and variable-slip methods relate to braking conditions with anti-lock brakes. The side-force tester is related to the lateral friction that occurs when the vehicle changes direction or compensates for cross-slope and cross-wind effects. The friction measuring devices used in this thesis are discussed below.

2.1.1 Locked-Wheel Trailer

The (ASTM E-274-97) locked-wheel trailer is the friction measuring device most used by state DOTs in the United States. It measures the steady-state friction force on a locked wheel over a wetted pavement surface as the wheel slides at a constant speed. The device consists of test wheels mounted on a trailer towed by a vehicle. The apparatus contains a transducer, instrumentation, a water supply system, controls for locking the test wheel, and a computer. During the test, the tow vehicle reaches the desired speed, water is delivered ahead of the test tire, and the braking system is activated to lock the test tire. The

resulting friction force acting between the test tire and the pavement surface, the normal force, and the speed of the test vehicle are recorded with the aid of suitable instrumentation. The wheel remains locked for approximately 1.0 s and the data are measured and averaged. The skid resistance of the paved surface is reported as skid number (SN) (ASTM E-274-97) or friction number (FN) (AASHTO T 242). This friction number is the required force to slide the locked test tire at a stated speed, divided by the effective wheel load and multiplied by 100 (ASTM E-274-97). The calculation of the skid number is described in Equation 2.1:

$$SN = \left(\frac{F}{W}\right) \times 100 \tag{2.1}$$

Where:

SN = skid number or friction,

F = tractive force or friction force, and

W = normal force of the test wheel.

The test (ASTM E-274-97) is conducted using a smooth tire (ASTM E-524) or a ribbed tire (ASTM E-501). The test tire inflation pressure is set at 24 psi (165 KPa). Pavement friction measurements can be conducted at different speeds. The standard test speed is 40 mph (64 kph). Figure 1 shows two examples of locked-wheel trailers.

(a) PN DOT

(b) CT DOT

Figure 1. Examples of ASTM E-274-97 Locked-Wheel Trailers

The average skid number recorded over the sections is typically reported. This device can also be set to detect peak friction values because the data are continuously recorded during the time that the tire is locked. One limitation of this system is that it does not measure continuously, and low-friction areas may

go unnoted when the tire is intermittently locked for measurements at specific locations along the road. This investigation used two computerized locked-wheel devices owned by the Virginia Department of Transportation (VDOT) and equipped with a smooth tire. Figure 2 shows the tire and water supply system.

Figure 2. Details of the Water Supply System

VDOT uses a smooth tire because it has been observed that friction measurements using this type of tire are more sensitive to surface microtexture and macrotexture. Also, smooth-tire measurements correlate better with wet-pavement crashes than do ribbed-tire measurements. However, some agencies are reluctant to use the smooth tire, possibly because the pavement friction results are lower than with the ribbed tire. The standard ribbed tire has groves that provide larger flow areas than surface macrotexture for water flow. As a result, the ribbed-tire measurements are less sensitive to surface macrotexture. Furthermore, since the ribbed tire is the original standard tire for this friction test, changing to a smooth tire would produce data that could not be compared with data measured in the past (Henry, 2000).

2.1.2 Dynamic Friction Tester

The dynamic friction tester (DFTester), shown in Figure 3, is a portable static device that can be used in the laboratory and in the field. The test procedure is described in ASTM E-1911-98. The device consists of a horizontal disk that spins in a plane parallel to the test surface. It has three rubber pads beneath the disk. When the disk reaches a tangential speed of 90 kph (56 mph), water is spread on the test surface and the disk is lowered to the surface of the pavement.

(a) Equipment in Use

(b) Bottom View of the Testing Pads

Figure 3. Dynamic Friction Tester (DFTester)

The torque is monitored by a transducer as the speed of the disk is reduced until it stops as a result of the friction between the pavement surface and the rubber pads. Friction measurements are typically recorded at speeds of 20, 40, 60, and 80 kph (12.4, 32, 64, and 50 mph). According to the manufacturer, the Dynamic Friction Tester has several advantages: measured values provide a continuous spectrum of dynamic coefficients of friction with good reproducibility, measurements can be made quickly, the device is easily transported because its design is compact and easy to carry, and the coefficient of friction at various speeds is recorded and reported. This enables users to create friction-speed curve gradients. One disadvantage of this device for field measurements is that measurements require traffic control.

The three rubber pads or sliders are pressed against the road surface by a vertical force (Figure 4). The horizontal force generated due to friction produces the torque that slows down the rotation of the disk. The coefficient μ, which varies in direct proportion to the horizontal force (F), can be obtained by Equation 2.2:

$$\mu = F/W \tag{2.2}$$

Where:

μ = coefficient of friction,

F = horizontal force, generated due to friction, and

W = constant load, perpendicular to the surface.

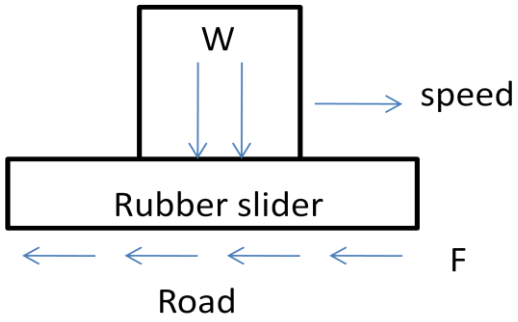

Figure 4. Measuring Principle of the DFTester

2.1.3 Circular Texture Meter

The Circular Texture Meter (CTMeter) is a portable device (shown in Figure 5) used to measure macrotexture in the lab or in the field (ASTM E-2157). The CTMeter has a charge-coupled device (CCD) laser mounted on an arm that rotates with a circumference of 890 mm (35 in). It is a lightweight apparatus that measures texture relatively quickly. The profile is measured on the same circumference that the DFTester uses to measure friction. Two different macrotexture indices can be computed from these profilers: mean profile depth (MPD) and root mean square (RMS). The MPD is a two-dimensional estimate of the three-dimensional Mean Texture Depth (MTD) and represents the average of the highest profile peaks occurring within eight 111.5-mm (4.4-in) individual segments included on the circle of measurement (Figure 6). The RMS is a statistical value that describes how much of the measured profile data deviates from a best-fit (modeled profile) of the data (Flintsch et al., 2003).

(a) Equipment in Use

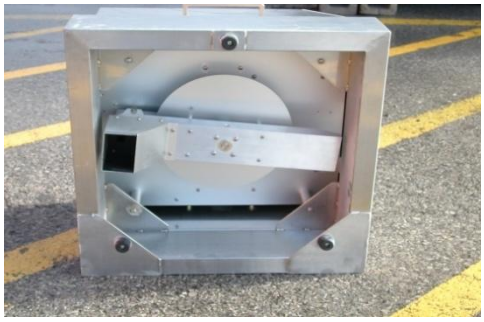

(b) Bottom View of the CCD Laser

Figure 5. The CTMeter

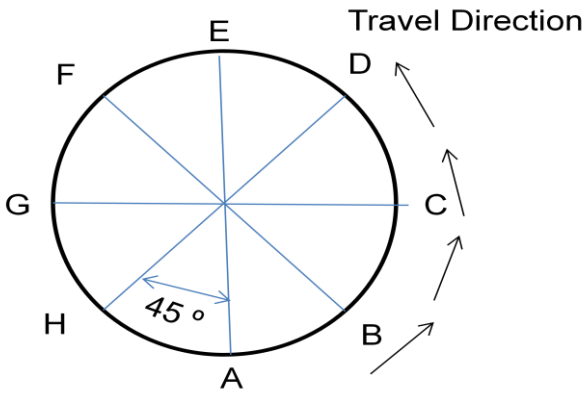

Figure 6. Segments of the Circular Texture Meter

The CTMeter is controlled by a notebook computer, which also performs the calculations and stores the measurements for each segment. The average for all eight segments and the overall average for all measurements in the pavement section evaluated are computed. Caltrans (2007) recommends the use of the average of the eight segments to produce a single value for each test location.

2.2 Fundamentals of Tire-Pavement Friction

Pavement friction is the force that resists the relative motion between a vehicle tire and a pavement surface. This resistive force is generated when the tire rolls or slides over the pavement surface (Li et al., 2004).

Since the rubber used in the tires is a visco-elastic material, tire-pavement friction does not obey the classical laws of friction. Friction between the tire and the rigid surface is not constant and is strongly dependent on tire pressure, temperature, and velocity. For example, low inflation pressure causes a reduction of friction at high speeds (Henry, 1983). Figure 7 illustrates how the friction force is the result of two main components shown in Equation 2.3 (Meyer and Kummer, 1967):

$$F\mu = Fa + Fh \tag{2.3}$$

Where:

$F\mu$ = friction force,

Fa = adhesion force component of the tire-pavement friction, and

Fh = hysteresis force component generated by the damping losses within the rubber.

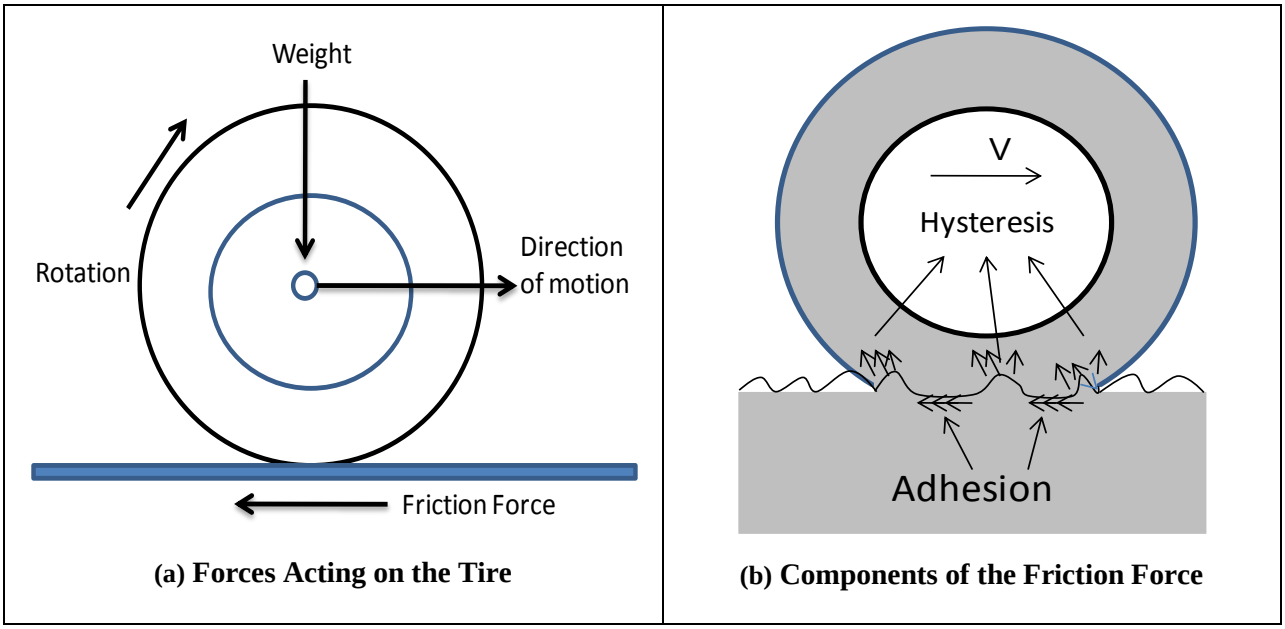

(a) Forces Acting on the Tire

(b) Components of the Friction Force

Figure 7. Tire-Pavement Friction Illustration

When the pavement surface is dry and smooth, adhesion force is the main contribution to the total friction force. This adhesion force is generated due to the molecular bonds between the rubber tread and the contacting area just below the surface (Li et al., 2004). On wet pavements the contact between the tire and pavement is affected by the water on the pavement. Under these conditions appropriate macrotexture is needed to allow for the rapid drainage of water from the tire-pavement interface. The enhanced drainage improves the contact between the tire and the pavement surface and helps reduce the probability of hydroplaning (Flintsch et al., 2003). On rough surfaces the tire tread will experience continuing deformation of compression and relaxation. In the compression phase, the deformation energy is stored within the rubbed tread. In the relaxation phase, part of the stored energy will be recovered and part of the stored energy will be lost in the form of heat, which is irreversible and identified with hysteresis losses (Li et al., 2004).

2.4 Pavement Surface Texture

Pavement texture has a very significant impact on tire-pavement friction. Pavement surface texture is composed of different combinations of texture depths (amplitude) and wave lengths. Pavement surface texture is affected by aggregate texture and gradation, pavement finishing techniques, and pavement wear, among other factors.

Texture is the pavement surface property that ultimately controls most vehicle-pavement interactions. Figure 8 illustrates the Road World Association (PIARC) pavement surface characteristics classifications and their impact on pavement performance measures.

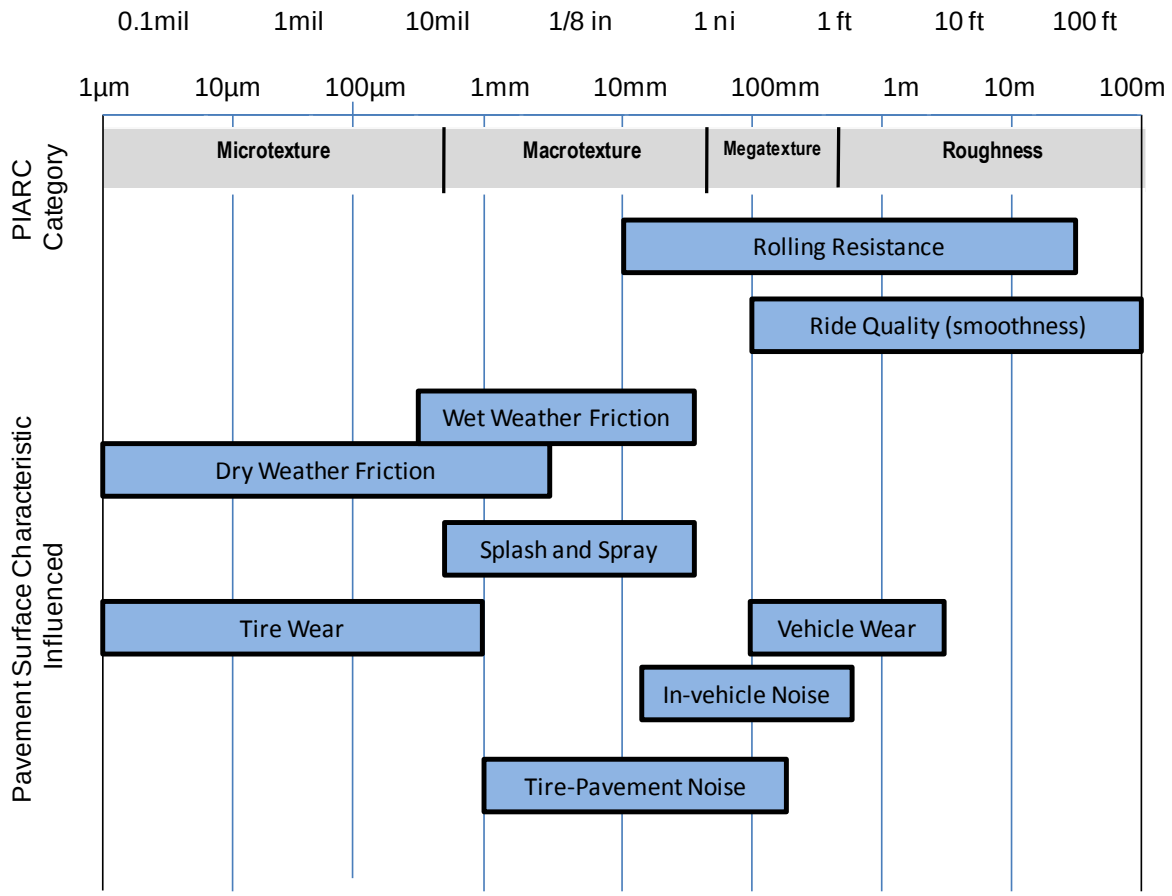

Figure 8. Pavement Surface Characteristics Classification and their Impact on Pavement Performance Measurements

The two main components of pavement texture that influence friction are microtexture (having wavelengths of 1 µm to 0.5 mm) and macrotexture (having wavelengths of 0.5 mm to 50 mm). High macrotexture generally reduces the potential for hydroplaning, improves the control at the tire and pavement surface footprint, and increases friction at higher speeds. On the other hand, microtexture has a stronger influence on friction at low speeds. The adhesion component of tire-pavement friction is related mostly with microtexture, while hysteresis is primarily associated with macrotexture. As the depth of the surface texture increases, the adhesion force decreases (because the contact area is reduced) and the hysteresis force component increases. Good microtexture is usually all that is needed to provide adequate stopping on dry pavements. At higher speeds (greater than 50 mph [80 kph]) on wet pavements good macrotexture is needed to allow the flow of water and to help minimize hydroplaning. When hydroplaning occurs, the entire footprint of the tire is separated from the pavement by a layer of water. As a result pavement surface contact is lost and the friction process is affected (Caltrans, 2007). Good

macrotexture and microtexture are needed to maintain adequate wet-pavement friction at all speeds (Flintsch et al., 2003).

2.5 Friction Indices and Models

Friction indices were first introduced in 1965 as an alternative to the coefficient of friction. ASTM started the use of skid number as a friction index (ASTM E-274). The American Association of State Highway and Transportation Officials (AASHTO) then adopted the ASTM E-274-97 test method and changed the terminology from skid number to friction number, in the standard AASHTO T 242. In the early 1990s PIARC developed the International Friction Index (IFI) based on a harmonization study conducted in several countries.

Pavement friction measurements are highly dependent on test speeds. Therefore, in order to compare friction properties using different equipment and speeds, it is necessary either to measure friction at two different speeds at least or to measure other surface properties such as macrotexture. Models proposed to describe the relation between friction and speeds include the Penn State, Rado, and International Friction Index (IFI) models.

2.5.1 The Penn State Model

Researchers at the Pennsylvania State University (Penn State) proposed one of the first models to describe the relationship between friction (μ) and speed (S). Leu and Henry (1976) proposed the model presented in Equation 2.4.

$$\mu = \mu_0 e^{\frac{-PNG\,(S)}{100}} \tag{2.4}$$

Where:

μ = friction,

μ_0 = intercept of friction at zero speed,

S = slip speed, and

PNG = percent normalized gradient.

Henry (2000) indicated that PNG is highly correlated with macrotexture and that μ_0 can be calculated from microtexture. Equation 2.4 was modified later by replacing the term (PNG/100) by a speed constant, Sp, resulting Equation 2.5.

$$\mu = \mu_0 e^{\frac{S}{Sp}} \quad (2.5)$$

Li et al. (2004) verified that Equation 2.5 accurately predicts friction after the wheel is locked and the braking continues.

2.5.2 The International Friction Index (IFI)

A series of international experiments were conducted by the World Road Association (PIARC) in several countries to compare and harmonize the test results obtained from various friction and macrotexture measuring devices. One of the products of these experiments is the International Friction Index (IFI). This model is an extension of the Penn State model.

The IFI is composed of two numbers: the friction number (F_{60}) and the speed constant (Sp). The friction number (F_{60}) indicates friction at a slip speed of 60 kph. It is a harmonized friction value, adjusted for the speed at which the test was performed and the type of device used. The speed constant (Sp) measures the speed dependency of the friction measurements, which is calculated based on the macrotexture of the pavement.

The IFI can be calculated (in metric form, according to the ASTM E-1960-07) as follows:

1. Measure the pavement friction FR(S) at a given slip speed S (in kph) using a selected friction device on the pavement macrotexture measured using a selected texture measuring device (e.g., the MPD in accordance with ASTM E-1845).
2. Estimate the IFI speed constant Sp using the MPD (TX) measured by the selected texture device according to Equation 2.6:

$$Sp = 14.2 + 89.7\ x\ TX \quad (2.6)$$

Where:

TX = macrotexture measured as MPD (mm).

3. Convert FR(S) at slip speed S to the corresponding friction at 60 kph using Equation 2.7:

$$FR(60) = FR(S) x\, e^{\left(\frac{S-60}{Sp}\right)} \quad (2.7)$$

Where:

FR (60) = friction value *FR(S)* at a slip speed of 60 kph,

FR (S) = friction value at selected slip speed *S*, and

S = selected slip speed (kph).

4. Calculate the IFI friction number [*F* (*60*)] using Equation 2.8:

$$F(60) = A + B\ x\ FR(60) + C\ x\ TX \quad (2.8)$$

Where:

A, B, C = calibration constants for the selected friction device, determined in accordance with ASTM E-1960-07.

The value of C is 0 when a smooth tire is used for the test; however, the term C × TX is necessary for ribbed tire tests because these tires are less sensitive to macrotexture (Wambold and Henry, 1996).

2.5.3 The Rado Model

This model captures friction proceeding from free rolling up to the locked-wheel condition under braking. The friction increases from zero to a peak value and then decreases to the locked-wheel friction. The Rado model simulates the transient phase when the brakes are first applied up to some slip. Anti-lock brake systems release the brakes to attempt to operate around the peak values of friction (Wambold and Andresen, 1999). The model follows Equation 2.9:

$$\mu(S) = \mu\ peak\ e^{-\left[\frac{ln\left(\frac{S}{S\ peak}\right)}{C}\right]\text{^}2} \quad (2.9)$$

Where:

$\mu(S)$ = friction value,

μ_{peak} = peak friction value,

S_{peak} = slip speed at peak (typically 15 percent of vehicle speed), and

C = shape factor related to the harshness of the texture.

The Penn State model and the Rado model combined can be used to simulate stopping emergency situations. The Rado model is used at the beginning part of the braking until the peak value is reached; after that, the Penn State model is more appropriate.

2.6 Short- and Long-Term Environmental Effects on Pavement Friction

Friction measurements vary with weather-related conditions such as temperature and precipitation. These environmental conditions have both long- and short-term effects on pavement surface friction properties. Several research efforts have focused on modeling these effects. Hill and Henry (1982) proposed a mechanistic model to predict seasonal variation on friction intercept (SN_0) based on the

analysis of data collected in experimental tests performed in Pennsylvania from 1978 to 1980. Equation 2.10 presents the proposed model, which is graphically illustrated in Figure 9.

$$SN_0 = SN_{0R} + SN_{0L} + SN_{0F} \quad (2.10)$$

Where:

SN_{0R} = short-term weather-related component of the skid number intercept (seasonal variations due to environmental conditions),

SN_{0L} = long-term seasonal variation (pavement age variations), and

SN_{0F} = a measure of SN_{0F} that is independent of both short- and long-term variations.

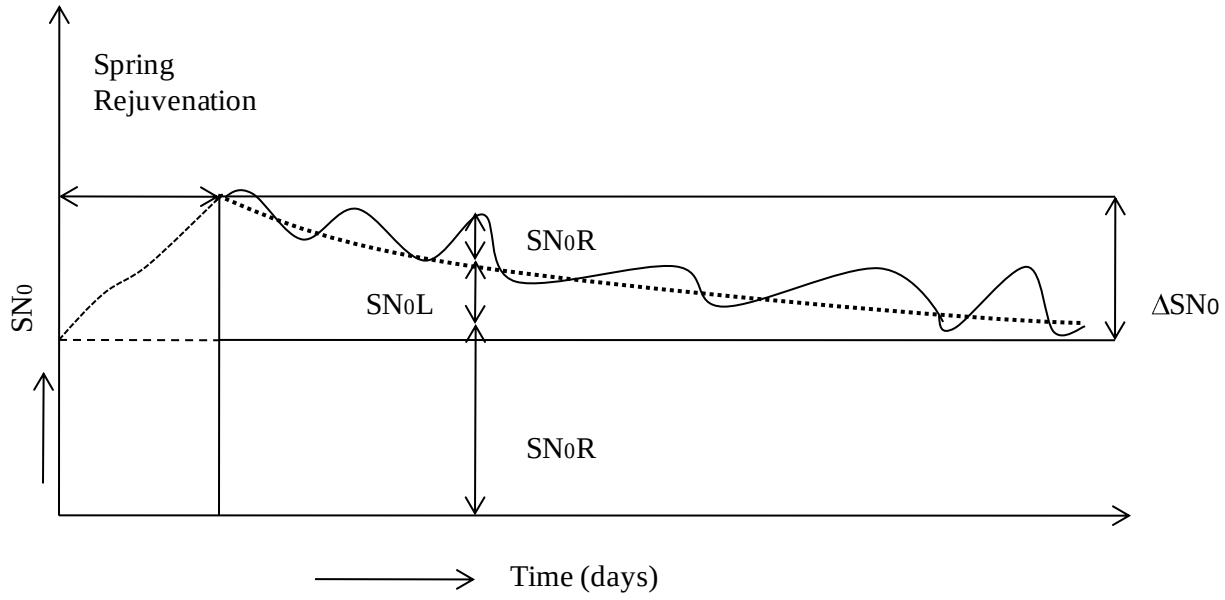

Figure 9. Mechanistic Model for SN_0

The long-term variation on asphalt surfaces was found to follow an exponential relationship as depicted in Equation 2.11.

$$SN_{0L} = \Delta SN_0 e^{-t/\tau} \quad (2.11)$$

Where:

ΔSN_0 = change in SN_0 over the testing season (year),

τ = rate at which long-term effects occur in asphalt surfaces, and

t = days from the beginning of test.

The parameters were found to depend on average daily traffic (ADT) and microtexture properties of the surface as indicated by Equations 2.12 and 2.13 (Hill and Henry, 1982).

$$\Delta SN_0 = 28.5 - 0.0023\ ADT - 0.09\ BPN \qquad (R^2 = 0.67) \qquad (2.12)$$

$$\tau = 67.67 - 0.0037\ ADT \qquad (R^2 = 0.28) \qquad (2.13)$$

Where:

BPN = British Pendulum Number, and

ADT = average daily traffic.

The short-term variation was found to be dependent on environmental factors, such as pavement temperature and dry days before the testing. The best-fit regression model is presented in Equation 2.14. It must be noted that the coefficient of determination very is low.

$$SN_{0R} = 3.79 - 1.17\ DSF - 0.104\ T_p \qquad (R^2 = 0.12) \qquad (2.14)$$

Where:

DSF = dry spell factor = ln (t_R + 1);

t_R = number of days since the last rainfall of 2.5 mm or more, $0 \leq t_R \leq 7$; and

T_p = pavement temperature (°C).

Once the short- and long-term variations in SN_0 have been calculated, Hill and Henry (1982) suggests that these parameters can be used to correct the SN at 64 kph (40 mph) following Equation 2.15.

$$SN_{64\,F} = SN_{64} - (SN_{0R} + SN_{0L})e^{-0.64\,PNG} \qquad (2.15)$$

Where:

$SN_{64\,F}$ = *SN* at 64 kph (40 mph) after removal of the short- and long-term effects, and

PNG = percent normalized gradient.

2.6.2 Seasonal Effects

Colony (1992) reported that friction fluctuates throughout the year with the lowest values occurring at the end of the summer and the highest values during the winter. A variation of approximately 30 percent of skid resistance has been observed in New Zealand between the minimum and the peak values throughout the seasons (Donbavand and Cook, 2004). Thus, pavements that provide satisfactory friction in the winter may not have adequate values during the summer. In general, it is believed that the effect of temperature on rubber resilience exerts a noticeable impact on all friction measurements (Meyer and Kummer, 1967). However, rubber composition has changed with time. Most available literature

reports lower friction at higher temperature than at low temperature. Furthermore, the magnitude of the variation of friction with temperature varies considerably from road to road, mainly because of the changes in road surface texture (Li et al., 2004). In addition to pavement temperature, Caltrans (2007) found that winter conditions and winter maintenance operation tend to increase aggregate microtexture, sometimes leading to a higher friction number in the spring and early summer rather than in late summer or fall. Other parameters that influence friction are periodic precipitation, aggregate polishing under traffic, and dust and oil accumulation, which accumulates on pavements during dry periods and might reduce the skid resistance numbers (AUSTROADS, 2004). Faung and Hughes (2007) observed that friction measurements on Superpave mixes with a nominal maximum aggregate size between 9.5 mm and 12.5 mm follow a cyclical pattern due to seasonal variation: friction measurements are higher in the winter and lower in the fall and summer.

2.6.1 Temperature Effects

In order to quantify the effect of temperature on friction pavements, four different temperatures must be taken into consideration: air (T_a), water (T_w), tire (T_t) and pavement temperature (T_p). However, all of them are correlated. For example, Runkle and Mahone (1980) found that water temperature and pavement temperature were highly correlated. Hill and Henry (1982) found that air, water, and pavement temperatures are also highly correlated.

Table 1 summarizes some of the main investigations. Kummer and Meyer (1962) present one of the first investigations of the effect of temperature on friction measurements. The study found that friction using the British Pendulum Tester decreases with higher temperatures.

Dahir and Henry (1979) found that the short-term component of the skid number measurements SN_{0R} decreases with increasing temperature (Equation 2.16). Elkin et al. (1980) also found a similar trend using a locked-wheel trailer in Indiana.

$$SN_{0R} = 5.09 - 0.232\ T_p \qquad (R^2 = 0.25) \qquad (2.16)$$

Where:

T_p = surface pavement temperature (ºC).

Table 1. Reference List of Different Temperature Formats Used in Studies

Source	Study Location	Type of Temperature	Friction Parameter	Effect of Temperature on Friction
Kummer and Meyer (1962)	Florida	slider rubber temperature	BPN	Coefficient decreases with temperature
Giles, Sabey, and Cardew (1964)	London	Ta	Friction Coefficient	Significant temperature effect
Tung, Henry, and Dahir (1977)	Pennsylvania	T_p and average and maximum Ta (day and night time)	SN_0	SN_0 decreases with temperature
Hill and Henry (1978)	Pennsylvania	T_p	SN_{0R} (Short term SN_0)	SN_{OR} decreases with temperature
Dahir and Henry (1979)	Pennsylvania	T_p	SN_0	SN_0 decreases with temperature
Burchett and Rizenbergs (1980)	Kentucky	average T_a during 4 to 8 weeks before test	SN_{40}	SN_{40} decreases with temperature
Runkle and Mahone (1980)	Virginia	maximum, minimum, and average T_a on the test day or in one week before test	SN_{40}	SN_{40} decreases with temperature
Elkin, Kercher, and Gulen (1980)	Indiana	T_p	SN_{40}	SN_{40} decreases with temperature
Anderson, Meyer, and Rosenberger (1984)	New York, Virginia, Pennsylvania	T_a during testing	SN_{40}	Significant temperature effect
Mitchell, Phillips, and Shah (1986)	Maryland	T_a during testing	SN_{40}	No significant effect observed
Oliver, Tredrea, and Pratt (1988)	Australia	T_p and T_t	SFC & SRV	SFC & SRV decrease with temperature
Jayawickrama and Thomas (1998)	Texas	T_a during testing (24 hr / 5 days)	SN_{40}	SN_{40} decreases with temperature
Luo, Flintsch, and Al-Quadi (2004)	Virginia	pavement temperature	SN_0 & PNG	SN_0 and PNG decrease with temperature
Wilson (2006)	New Zealand	seasonal variation	SN	Significant variation
de Solminihac and Echaveguren (2007)	Chile	daily temperature oscillations and speed	GT	Skid resistance values measured are higher in the warm seasons
Faungs and Hughes (2007)	Virginia	seasonal variation	SN	Maximum SN values during the winter, minimum values in summer or fall

Oliver (1980) studied seasonal friction variations in Australia using a British Pendulum Tester (BPN). The researcher tested a set of laboratory-prepared surfaces similar to normal pavement surfaces. The skid resistance range covered values from 15 to 90 units and a range of surface textures between 0 and 1.5 mm (0 to 0.0059 in). These surface samples were tested outdoors with temperatures variation from 7 to 59 ºC (45 to 138°F). The study found a good correlation between friction and temperature (Equation 2.17).

$$SRV_T/SRV_{20} = 1 - 0.00525 * (T - 20) \quad (2.17)$$

Where:

T = prepared pavement surface temperature (ºC),

SRV_T = the skid resistance value obtained at temperature T (ºC), and

SRV_{20} = the skid resistance value obtained at 20ºC.

Oliver et al. (1988) studied the effect of tire temperature and found that cornering friction decreased with temperature in accordance to Equation 2.18 with a high coefficient of determination. The research also showed that the tire temperature is proportional to the air temperature and pavement temperature (Equation 2.19)

$$SFC_T / SFC_{25} = 0.563 + 45.9/(T+80) \qquad (R^2 = 0.83). \quad (2.18)$$

$$T = 12.3 + 0.48*(T_a+T_p) \quad (2.19)$$

Where:

SFC_T = side force coefficient of SCRIM at tire temperature T,

T = tire temperature (°C),

T_a = air temperature (°C), and

T_p = pavement temperature (°C).

The researchers concluded that both air and pavement temperature determined the rubber temperature, which affects the viscoelastic properties of the rubber (Oliver, Tredrea, and Pratt, 1988).

In the United States, Jayawickrama and Thomas (1998) observed that the friction number at zero speed (FN_0) tends to decrease at higher temperatures. The researchers also hypothesized that temperature changes affect the rubber tire properties used in the locked-wheel device for trailer measurements. Hysteresis is affected at higher temperature because the rubber becomes more flexible, leading to less

energy loss. As a result, higher temperature leads to smaller friction number measurements (Bazlamit and Reza, 2005).

Luo et al. (2004) found that pavement temperature measured 38 mm (1.5 in) below the surface has a significant effect not only on pavement friction measurements but also on the sensitivity of the measurements to the test speed. The study found that both the friction at zero speed (SN_0) and the percent normalized gradient (PNG) tend to decrease with increased pavement temperature. Figure 10 shows the general trend of change of SN_0 and PNG with pavement temperature. The decrease in SN_0 could be explained by a reduction in the exposed microtexture component of the pavement. Since the binder is softer at higher temperatures, it may cover more of the aggregate. Thus, the adhesion component of the tire-pavement friction is decreased. Since PNG also decreases with higher temperatures, the slope of the friction versus speed is flattened; as a result, an inverted effect at higher speeds is observed (friction increases with higher temperature at higher speeds). This makes the effect of temperature on friction dependent on the testing speed. For a standard 9.5-mm Superpave wearing surface mix, the research showed that pavement friction tends to decrease with increased pavement temperature at low speeds. At high speeds, the effect for the same mix is inverted, and pavement friction tends to increase with increased pavement temperature.

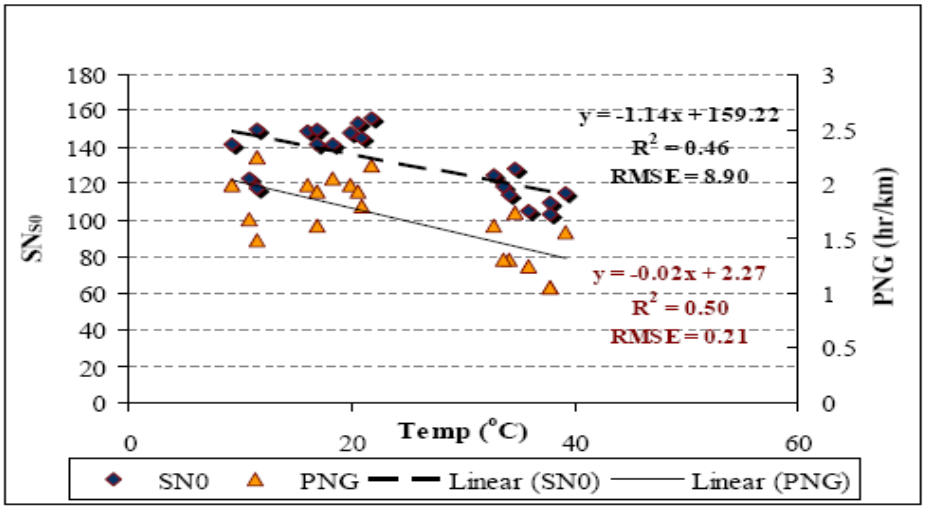

Figure 10. SN_0 and PNG versus Pavement Temperature (Luo and Flintsch, 2004)

(Figure obtained from the thesis: Effect of Pavement Temperature on Frictional Properties of Hot-Mix-Asphalt Pavement Surfaces at the Virginia Smart Road, studied by Luo and Flintsch, January 2003)

Luo et al. (2004) developed the following temperature-dependent friction models for a 9.5-mm Superpave binder wearing surfaces prepared with a PG 64-22 binder.

$$SNS(T) = (159 - 1.14T) * e^{-\left\{\frac{2.27-0.02T}{100}\right\}*V} \quad (2.20)$$

$$SNR\,(T) = (118 - 73T) * e^{-\left\{\frac{1.00-0.01T}{100}\right\}*V} \quad (2.21)$$

Where:

$SN_s\,(T)$ = skid number using the smooth tire for SM 9.5D at temperature T,

$SN_R\,(T)$ = skid number using the ribbed tire for SM 9.5D at temperature T,

T = pavement temperature 38.1 mm (1.5 in) below the surface, and

V= speed (kph).

De Solminihac and Echaveguren (2007) observed that skid resistance values measured with a Griptester at 50 kph (31 mph) are affected by daily temperature oscillations, traffic conditions, and speed. The researchers proposed an adjustment factor to standardize values measured under different temperature conditions during the summer months.

2.7 Summary

Wet-pavement friction measurements can be measured using different devices, including laboratory and field equipment. These devices use different principles and produce different friction values. The two main components of friction are adhesion and hysteresis, and both are related to pavement surface texture. Adhesion is affected mostly by the microtexture properties of the pavement surfaces, and hysteresis is affected mostly by the macrotexture. Good macrotexture and microtexture are needed to maintain adequate wet-pavement friction at all speeds.

Pavement friction measurements are affected by many seasonal (environmental) factors. These measurements experience short- and long-term variations. The long-term variation is caused mostly by traffic. The short-term variations are caused mostly by changes in environmental conditions, such as pavement temperature and dry days before the test. The general trend is that friction measurements are higher in the winter and early spring than during the summer.

CHAPTER 3. EXPERIMENTAL PROGRAM

This thesis investigated the changes in friction properties on nine flexible pavement sections over a period of two years. This chapter presents a detailed description of the sections evaluated and the friction measurements conducted for this study.

3.1 The Virginia Smart Road

The Virginia Smart Road is the first stage of a 9.6-km (5.84 mi) connector highway between Blacksburg and I-81 in southwest Virginia. It is a 3.2-km (2-mi) controlled test track that is used for transportation research, including pavement surfaces properties. The road has two lanes and is composed of many pavement sections with different types of surfaces.

The facility includes 12 experimental flexible pavement test sections and two rigid pavement sections. The flexible pavement sections are approximately 100 m long and were built with different hot-mix asphalt (HMA) wearing surfaces: four Superpave mixes designed with different aggregate structure and binder types and three experimental mixes. The three experimental mixes include an open graded friction course (OGFC) section and two stone matrix asphalt (SMA) sections. The concrete sections include a continuously reinforced concrete pavement (CRCP) and a jointed plain concrete pavement (JPCP). The CRCP and JPCP sections have a transversely tined surface, and the JPCP has received localized longitudinal diamond grinding. Two sub-sections of the CRCP have been overlaid with epoxy-based surface treatments.

3.2 Experimental Design

This thesis considered nine HMA surfaces. Examples of these surfaces are shown in Figure 11. The specific surface mix types used in this study, their characteristics (aggregate nominal maximum size, binder) and the completion dates are shown in Table 2. The surface mixture type SM 9.5D is the most-used mixture on interstate highways in Virginia.

Although friction and texture measurements were also conducted on the two Portland concrete cement (PCC) sections (CRCP and JPCP) and on two special surface sections (Cargill and EP-5), only the measurements on the flexible pavement sections were included in this investigation.

(a) SM 9.5D Superpave **(b) OGFC** **(c) SMA 9.5D**

Figure 11. Sample of HMA Pavement Surfaces Available at the Smart Road

Table 2. Wearing Surface Mixes Used at the Virginia Smart Road

Section	Mix Denomination	Aggregate Nominal Maximum Size NMS	Binder	Completion Date
Loop	SMA	12.5	PG 76-22	11/09/99
A	SM 12.5D	12.5	PG 70-22	11/11/99
B	SM 9.5D	9.5	PG 70-22	11/11/99
C	SM 9.5E	9.5	PG 76-22	11/12/99
D	SM 9.5A	9.5	PG 64-22	11/10/99
I	SM 9.5A	9.5	PG 64-22	11/08/99
J	SM 9.5D	9.5	PG 70-22	11/08/99
K	OGFC	9.5	PG 76-22	26/05/06
L	SMA-12.5	12.5	PG 76-22	11/09/99

The HMA surface mix (SM) denomination includes the maximum size of the aggregate (the number written with the SM) and a letter (A, D, or E) that denotes PG grading of the binder used (PG 64-22, 70-22, and 76-22, respectively). Four of the listed surface mixes were experimental at the time of construction: (1) section I, which was designed using 75 gyrations instead of the standard 65 used by VDOT; (2) section K, with an OGFC; and (3) Loop and (4) section L with an SMA.

Because the Virginia Smart Road (Figure 12) is a research facility that is not open to regular traffic, the surface friction characterization should not change significantly due to traffic weathering. This provides a unique opportunity to isolate friction variations due to environmental conditions. Each section was tested in both lanes because they were constructed at different times. Thus different measurements of friction may be obtained for each of the sections in different directions.

Figure 12. Aerial View of the Virginia Smart Road

3.3 Test Procedures

Friction tests were conducted using two locked-wheel trailers (ASTM E-274-97) with smooth tires (ASTM E-524) and a DFTester (ASTM E-501). VDOT owns two locked-wheel trailers: an analog and a digital device. The digital one is a newer version of the analog locked-wheel trailer. Friction measurements with the locked-wheel trailers and the DFTester were conducted on the same day. Macrotexture was measured with a CTMeter (ASTM E-2157) two weeks after the friction tests. Measurements on nine HMA sections and two PCC sections were tested on both lanes (eastbound and westbound). Friction and macrotexture experiments were carried out monthly beginning in December 2006 and ending in July 2008. The test procedures utilized for this investigation are described below.

3.3.1 Locked-Wheel Trailer

Skid resistance tests using the locked-wheel trailer were conducted at three speeds: 32, 64, and 80 kph (20, 40, and 50 mph) using a smooth tire. Tests were repeated three times for each speed and direction. Figure 13 shows a site layout with the specific locations of the measurements.

Usually, Friction numbers are reported as “FN” followed by the test speed, followed by a letter “R” if a ribbed tire was used or “S “if a smooth tire was used. If the test speed is expressed in kph, the number is enclosed within parentheses. For example, “FN (64) S” would mean that the test was conducted at 64 kph using a smooth tire.

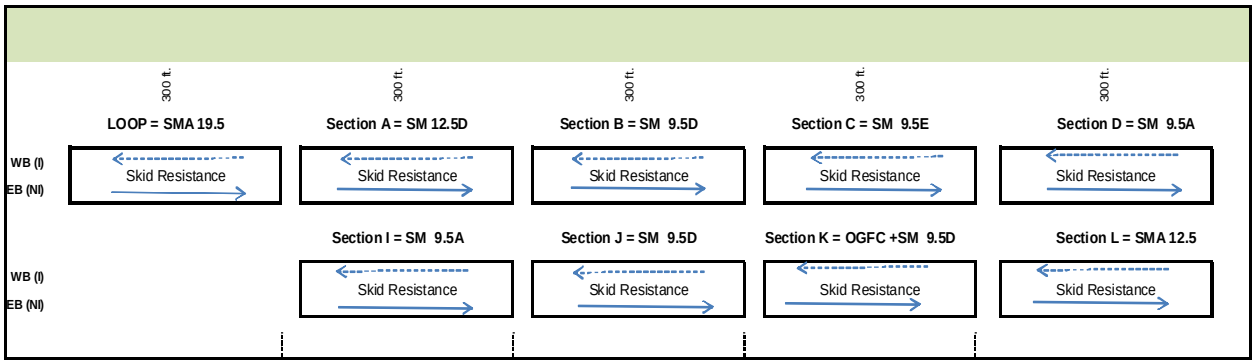

Figure 13. Locations of Skid Resistance Measurements

Table 3 presents an example of a raw data collected by the locked-wheel device for all sections at 64 kph (40 mph) in June 2007. The first three columns are the reference position of the trailer in miles and feet, respectively, and the section tested. The next two columns are the average and standard deviation for the measured FN. The last two columns are the average and standard deviation of the speed at which the test is conducted.

Table 3. Example of Raw Data Collected by the Locked-Wheel Trailer

File			E20.E03			
Date			06/22			
Time			10:22			
REF			*FN*		*SPEED (mph)*	
POST	*FEET*	*Section*	*AVG*	*STD*	*AVG*	*STD*
0.000	0		DM1_ON			
0.008	42	Loop	**76.8**	1.18	20.5	0.41
0.061	322	A	**74.4**	0.80	20.3	0.24
0.126	665	B	**74.7**	1.03	20.7	0.42
0.187	987	C	**72.2**	1.25	21.5	0.36
0.248	1309	D	**64.3**	1.15	21.1	0.06
0.595	3142	I	**75.8**	1.02	19.8	0.29
0.648	3421	J	**75.3**	1.19	19.6	0.06
0.713	3765	K	**61.3**	0.93	21.9	0.14
0.790	4171	L	**67.4**	1.20	21.6	0.12
0.858	4530	Cargill	**71.9**	2.66	21	0.21
0.939	4958	EP5	**59.3**	1.26	20.9	0.14
0.975	5148	CRCP	**65.5**	2.37	20.5	0.13

Periodic calibration of the locked-wheel trailer assured accuracy of the data obtained in tests. Calibration requirements include calibration of the speed and calibration of the skid resistance force (ASTM E-274-97). Speed transducer measurements must provide speed resolution and accuracy of

±1.5 percent of the indicated speed or ±8 kph (±0.5 mph). Force and torque transducers most provide an output directly proportional to torque with hysteresis less than 1 percent of the applied load and nonlinearity up to the maximum expected loading of less than 1 percent of the applied load. The calibration of the analog and the digital devices occurred on April 2007 and April 2008, respectively.

3.3.2 Dynamic Friction Tester (DFTester)

Monthly DFTester measurements were conducted in accordance with ASTM E-1969. The friction was recorded at four speeds: 20, 40, 60, and 80 kph (12.4, 20, 40, and 50 mph). The test results are recorded and plotted against speed by the system, as shown in Figure 14.

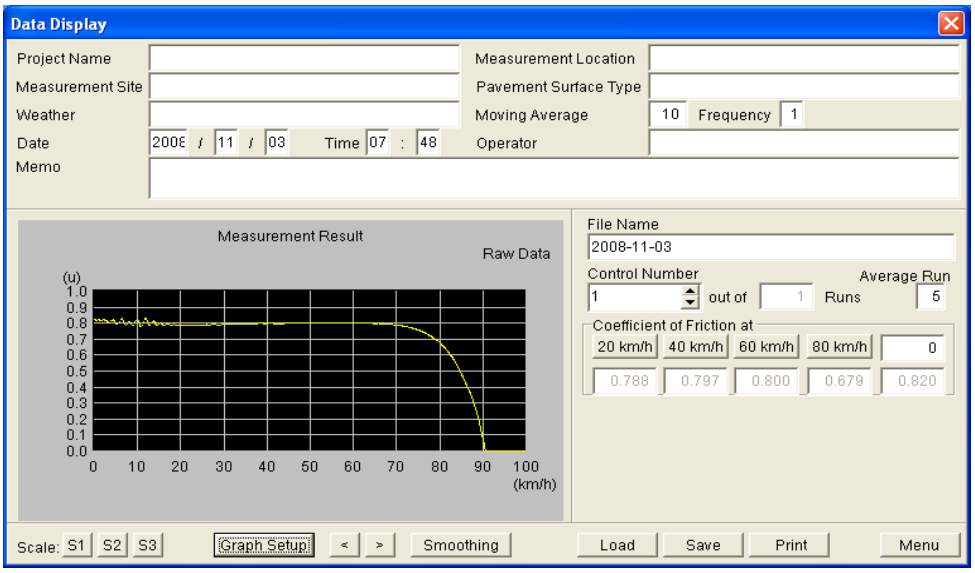

Figure 14. Example of a Raw Friction Measurement Taken by the DFTester

Friction was measured on three pre-selected locations in each section and lane. Thus a total of six measurements were taken on each section, three on each lane. Figure 15 shows the pre-selected locations on the various sections. These spots were marked on the road to allow testing on the same location every month. In order to take into account the effect of temperature, the sequence of the experiment was established by measuring two pre-selected locations at a time on each of the sections. The test started on section L and finished on section Loop. After completing this first set of measurements on each of the nine sections, the experiment was repeated for the second and third sets of pre-selected locations.

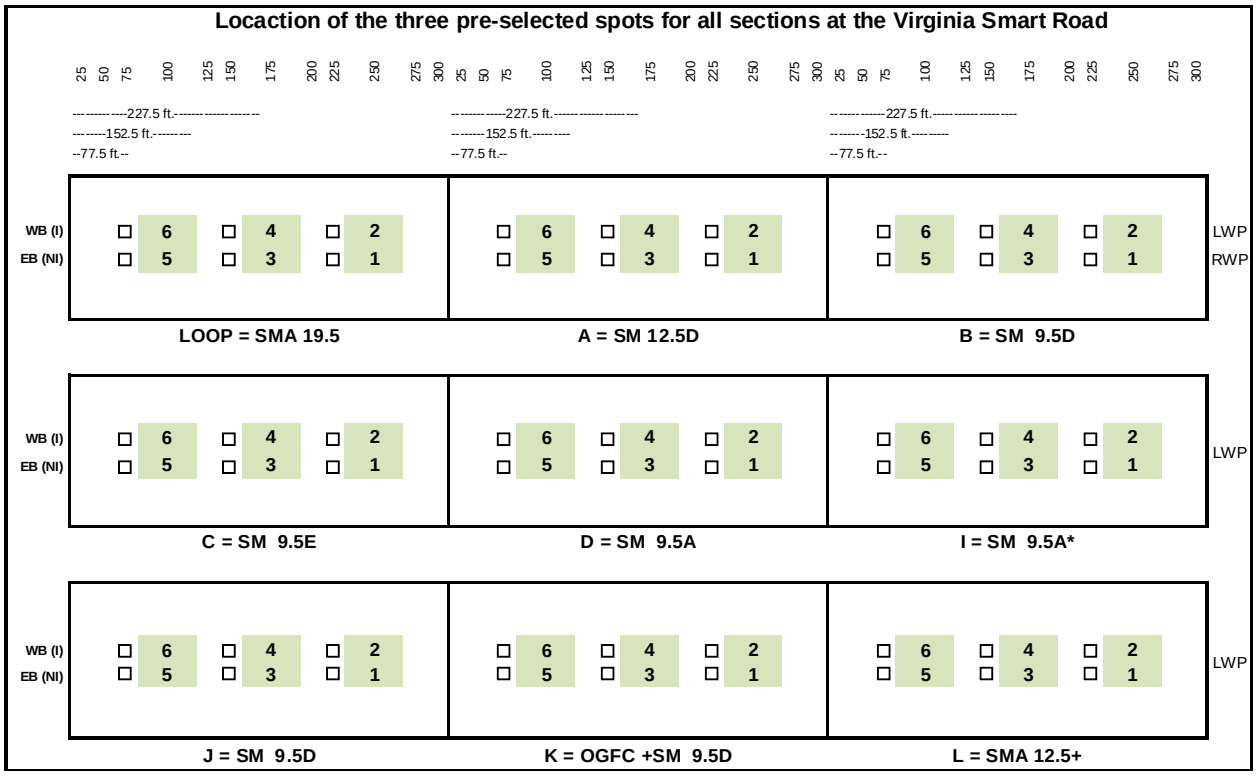

Figure 15. Specific Test Locations for the DFTester and the CTMeter Measurements

3.3.3 Circular Texture Meter (CTMeter)

Macrotexture measurements were taken monthly using the CTMeter on the same locations in which DFTester measurements were taken (Figure 15). For consistency, the apparatus was always placed oriented longitudinally to the road.

Figure 16 presents an example of the macrotexture values measured in section L in June 2008. The letters A through H denote the eight measurement segments. Numbers 1 through 6 denote the six pre-selected locations within the section. The overall average and standard deviation for the section (six locations) is calculated and displayed in the last three rows.

```
Texture Measurements June 2008
SECTION L
[1]-------------------------
 A:0.88(2%)[0.77]B:0.82(2%)[0.63]C:0.85(0%)[0.73]D:0.88(3%)[0.79]
 E:1.01(3%)[0.97]F:0.88(2%)[0.90]G:0.95(0%)[0.64]H:0.82(0%)[0.78]
 Ave: 0.89(2%)[0.78]
[2]-------------------------
 A: 1.03(3%)[0.81]B: 0.96(1%)[0.88]C: 0.79(0%)[0.68]D:0.84(1%)[0.59]
 E:0.65(2%)[0.44] F:0.62(2%)[0.53]G:0.94(4%)[0.76]H:0.92(2%)[0.78]
 Ave:0.84(2%)[0.68]
[3]-------------------------
 A:0.77(1%)[0.54]B:1.06(1%)[0.80]C:0.71(2%)[0.66]D:0.97(0%)[0.85]
 E:1.20(2%)[1.00]F:0.88(1%)[0.88]G:0.79(1%)[0.45] H:0.83(1%)[0.82]
 Ave:0.90(1%)[0.75]
[4]-------------------------
 A:1.16(3%)[2.63]B:0.95(5%)[0.77]C:0.92(1%)[0.93]D:0.99(4%)[0.81]
 E:  1.09(1%) [0.94] F:  1.27(2%) [1.38] G:  0.98(0%) [0.87] H:  1.11(1%) [0.83]
 Ave:1.06(2%)[1.15]
[5]-------------------------
 A:0.56(1%)[0.55]B:0.84(0%)[0.66]C:0.71(0%)[0.67]D:0.76(2%)[0.67]
 E:0.77(0%)[0.53]F:  0.73(1%)[0.68]G:0.62(0%)[0.42]H:0.80(0%)[0.56]
 Ave:0.72(1%)[0.59]
[6]-------------------------
 A:0.60(1%)[0.56]B:0.54(2%)[0.51]C:0.92(0%)[0.86]D:0.75(0%)[0.56]
 E:0.92(1%)[0.60]F:0.90(0%)[0.78]G:1.23(1%)[0.98]H: 0.79(0%)[0.58]
 Ave:0.83(1%)[0.68]
[Ave]-------------------------
 A:0.83(2%)[0.98]B:0.86(2%)[0.71]C:0.82(1%)[0.76]D:0.87(2%)[0.71]
 E:0.94(2%)[0.75]F:0.88(1%)[0.86]G:0.92(1%)[0.69]H:0.88(1%)[0.73]
 Ave:0.87(2%)[0.77]
```

Figure 16. Example of Raw Data Collected by the CTMeter

3.4 Air Temperature

Air temperatures for all test dates were obtained from the National Climatic Data Center (2008). Air temperature was recorded at the climatic station located at the Blacksburg airport, near the Virginia Smart Road. Available records include the maximum, minimum, and average temperature of the day, among other data. An extract of this table for the first days of June 2008 is shown in Figure 17:

Figure 17. Example of Temperature Data for June 2008

```
  TEMPERATURE IN F:        :PCPN:    SNOW:  WIND      :SUNSHINE: SKY     :PK WND
================================================================================
1   2   3   4   5  6A  6B    7    8   9   10  11  12  13   14  15   16   17  18
      Temperature                          AVG MX 2MIN
DY MAX MIN AVG DEP HDD CDD  WTR  SNW DPTH SPD SPD DIR MIN PSBL S-S WX    SPD DR
================================================================================

 1  77  58  68   5   0   3 0.14  0.0    0  4.0 10 270   M    M   3        21 320
 2  78  53  66   2   0   1 0.00  0.0    0  2.4 12 290   M    M   1        17 290
```

The average, maximum, and minimum temperatures are plotted against time in Figure 18. An approximately sinusoidal tendency is observed for the three temperatures. The hottest month of the year is August, which theoretically will correspond to the lowest friction measurement.

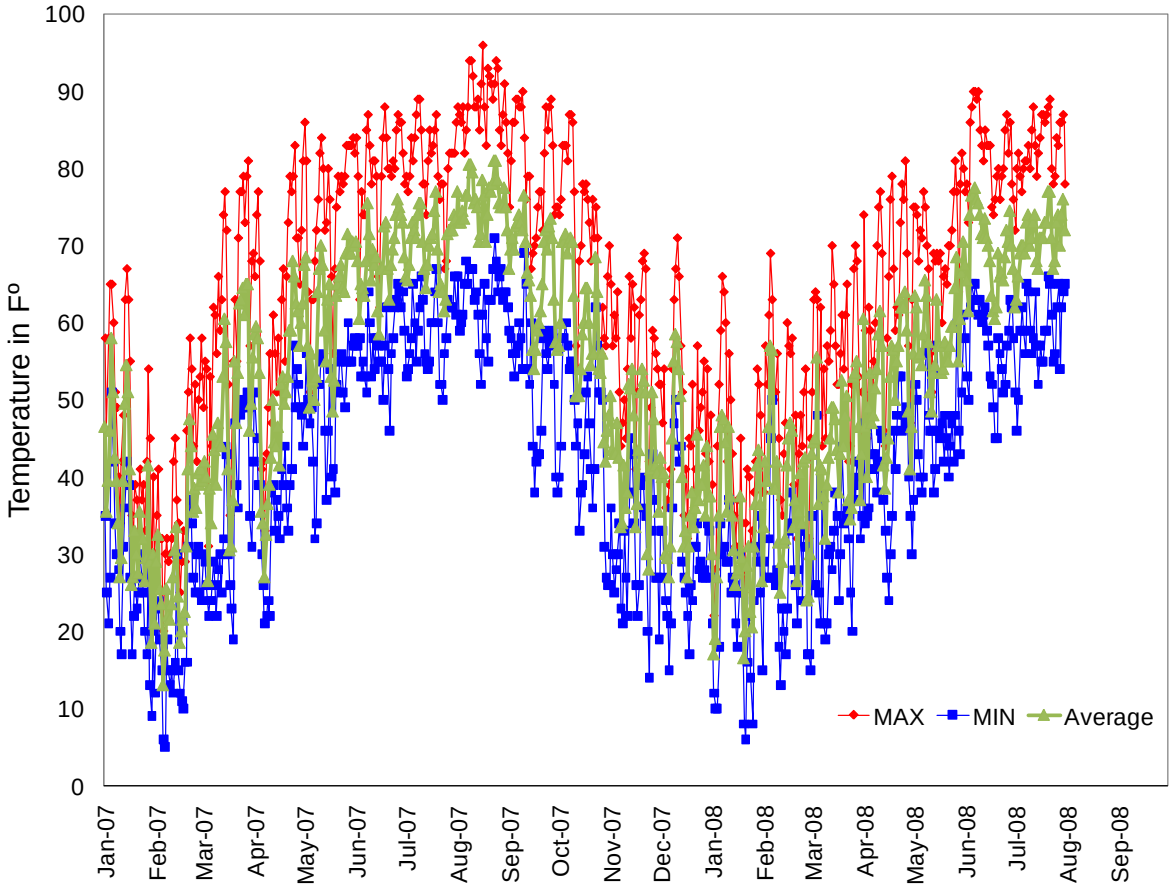

Figure 18. Blacksburg, Virginia, Year Temperature Variation

3.5 Summary

To evaluate the effect of seasonal variation on pavement surface friction, measurements of friction and texture on nine HMA sections at the Virginia Smart Road were conducted every month over a year and a half (from December 2006 to July 2008). Friction was measured using locked-wheel trailers and a DFTester. Both friction tests were conducted on the same day. Macrotexture measurements were taken using the CTMeter on the same locations where DFTester measurements were taken.

CHAPTER 4. DATA COLLECTION

This chapter presents the data collected to evaluate the effects of seasonal and temperature variation on pavement friction surface properties, including friction and macrotexture measurements.

4.1 Pavement Friction Measurements

4.1.1 Locked-Wheel Device

Pavement friction measurements using the locked-wheel trailers were conducted at three speeds: 32, 64, and 80 kph (20, 40, and 50 mph). The tests were repeated three times per speed and direction. An average of the three friction numbers at each speed was calculated and reported as the section friction number. Table 4, Table 5, and Table 6 show the average friction number measured using the locked-wheel trailer at 32, 64, and 80 kph (20, 40, and 50 mph), respectively. Because two different devices were utilized during the investigation, the data are divided in two categories: analog instrument data and digital instrument data. The analog device was utilized in February 2007, March 2007, August 2007, September 2007, November 2007, December 2007, and February 2008. The digital device was utilized for all the other months. Table 7 shows the average and the standard deviation for each section and device. There were some problems with device calibration in May 2008 that affected the friction correction factors for that month. The friction values for that month were not considered; however a good tendency is observed following the model correction factors for the month. The months considered for the data analysis are January 2007 through June 2008.

4.1.2 Dynamic Friction Tester Measurements

The DFTester measurements were performed in accordance with ASTM E-1969, and the friction was recorded at 20, 40, 60, and 80 kph (12.4, 32, 64, and 50 mph) respectively. Friction measurements were also determined for 32 and 64 kph (20, and 40 mph) using interpolation. The average of the three tests in each section and direction was computed, resulting in two friction average values, one per section (eastbound and westbound). The friction values for all sections and both directions are reported in Tables 8, 9, 10, and 11 for 20, 32, 64, and 80 kph (12.4, 20, 40, and 50 mph), respectively. The analyzed data includes friction measurements from May 2007 through July 2008. There were problems with the data collected during February and March 2008, so those data were not considered in the analysis.

Table 4. Average Monthly Friction Measurements Using the Locked-Wheel Device at 32 kph (20 mph)

Section	Date																	
	Feb 07	Mar 07	Aug 07	Sep 07	Nov 07	Dec 07	Feb 08	Dec 06	Jan 07	Apr 07	May 07	Jun 07	Jul 07	Oct 07	Feb 08	Mar 08	Apr 08	Jun 08
Eastbound 32 kph (20 kph) Analog Equipment								**Eastbound 32 kph (20 kph) Digital Equipment**										
Loop	79.1	74.6	76.7	79.9	77.9	76.4	75.6	74.9	75.9	82.7	77.0	82.0	82.3	84.0	74.6	75.3	77.3	75.7
A	78.4	78.2	71.8	76.7	77.1	79.3	76.3	76.8	77.6	77.1	n/a	76.6	79.2	76.5	77.1	78.6	79.6	78.2
B	81.4	80.6	76.5	77.5	79.3	79.7	73.7	81.3	81.9	81.8	73.4	75.0	80.6	78.9	79.0	79.0	82.4	76.1
C	79.5	75.9	72.6	75.2	74.0	75.4	72.7	78.5	77.7	77.6	n/a	76.1	78.7	74.3	77.2	73.3	78.0	76.2
D	70.5	70.8	61.5	65.1	67.4	67.0	66.6	77.2	70.3	67.2	65.4	70.5	69.1	69.9	71.6	71.2	72.6	66.5
I	79.0	77.8	75.3	75.9	77.2	77.8	76.5	79.5	78.6	79.5	n/a	79.3	79.2	69.5	78.0	76.1	80.1	77.5
J	80.8	77.3	78.1	78.2	78.0	76.5	76.1	76.8	73.9	81.7	60.6	79.5	79.6	81.2	74.6	74.0	79.0	75.6
K	57.0	59.9	66.0	63.4	63.5	64.2	62.6	57.0	54.0	64.1	n/a	67.7	68.2	65.7	64.8	60.6	64.1	63.9
L	74.2	71.4	69.5	67.0	69.7	68.4	65.2	70.2	65.4	71.7	69.4	70.7	71.9	n/a	67.4	67.5	70.9	65.7
Westbound 32 kph (20 kph) Analog Equipment								**Westbound 32 (20 kph) kph Digital Equipment**										
L	73.1	72.0	70.7	65.6	66.2	69.2	65.7	70.2	66.5	75.0	75.0	68.8	71.2	66.2	68.7	60.8	69.9	65.0
K	60.6	56.7	64.8	61.8	62.1	62.9	62.1	54.4	54.4	59.4	59.4	62.7	67.8	64.0	62.0	57.5	65.0	62.9
J	78.6	68.1	75.1	71.6	76.0	82.0	74.7	81.9	73.2	74.0	74.0	74.3	80.3	69.4	79.1	79.1	76.5	72.9
I	79.3	76.0	78.2	78.2	80.2	80.0	79.5	78.4	82.1	79.7	79.7	79.0	81.3	n/a	78.7	77.6	83.2	79.6
D	79.7	74.4	71.0	72.3	74.4	75.4	71.1	80.8	75.3	74.6	74.6	74.7	73.7	72.3	74.8	74.1	78.4	70.5
C	80.5	78.0	75.9	76.4	76.9	80.4	74.8	80.7	74.4	80.3	80.3	79.2	80.5	77.8	76.2	75.6	80.4	74.0
B	83.2	82.7	80.4	79.2	80.0	82.7	76.5	83.0	78.7	86.1	86.1	85.1	84.5	80.6	81.6	75.4	79.8	77.0
A	83.7	81.2	77.8	77.0	78.7	79.1	75.3	83.4	79.9	81.2	81.2	81.4	79.3	81.7	77.0	74.5	78.9	73.0
Loop	78.1	72.9	75.3	72.1	74.9	68.5	70.3	76.9	71.3	73.5	73.5	71.4	74.9	75.0	66.1	66.3	73.4	68.6

Table 5. Average Monthly Friction Measurements Using the Locked-Wheel Device at 64 kph (40 mph)

Section	Date																	
	Feb 07	Mar 07	Aug 07	Sep 07	Nov 07	Dec 07	Feb 08	Dec 06	Jan 07	Apr 07	May 07	Jun 07	Jul 07	Oct 07	Feb 08	Mar 08	Apr 08	Jun 08
Eastbound 64 kph (40 mph) Analog Equipment								**Eastbound 64 kph (40 mph) Digital Equipment**										
Loop	62.0	60.2	52.5	57.9	54.0	57.1	53.3	57.9	58.8	59.3	55.0	57.9	62.3	55.3	56.1	56.6	59.4	54.3
A	44.9	43.4	42.6	41.6	42.6	47.0	48.4	46.7	43.2	40.6	n/a	45.8	48.7	47.5	44.9	50.0	44.3	44.5
B	50.7	50.5	42.8	45.0	45.6	46.6	45.2	51.2	45.3	43.9	46.4	43.1	48.7	49.9	47.6	56.5	49.2	47.6
C	50.3	50.1	44.7	50.4	46.4	51.3	48.5	47.3	47.0	49.9	n/a	47.5	51.1	40.4	50.4	47.9	52.5	44.7
D	37.8	39.4	30.8	35.0	37.6	38.7	37.8	40.8	40.5	38.1	43.0	36.5	36.3	32.9	39.5	41.2	43.1	36.0
I	60.6	53.3	50.4	50.5	54.5	54.6	54.7	56.5	55.1	52.3	n/a	52.3	55.6	n/a	54.3	57.2	60.2	50.4
J	60.3	59.6	57.1	58.8	55.6	56.1	56.7	59.1	55.3	58.4	46.9	53.9	60.0	53.3	57.7	57.6	59.7	52.2
K	45.8	46.2	54.3	51.3	51.2	49.5	51.0	39.8	37.9	47.3	n/a	51.8	52.4	48.8	50.0	47.5	52.1	48.3
L	52.7	50.8	48.7	50.3	48.8	49.8	48.3	52.0	49.2	50.1	49.9	48.5	50.9	46.7	49.2	49.1	52.2	45.9
Westbound 64 kph (40 mph) Analog Equipment								**Westbound 64 kph (40 mph) Digital Equipment**										
L	54.0	48.9	49.3	50.5	49.0	52.2	49.3	52.6	46.9	53.8	52.8	48.6	51.8	45.5	49.2	49.9	51.9	48.8
K	46.1	43.1	54.1	52.6	50.9	49.9	51.4	41.7	42.1	45.6	n/a	47.3	53.1	50.8	49.8	46.1	52.0	49.1
J	48.5	46.3	49.2	46.7	50.4	55.3	51.0	52.6	45.4	51.9	48.3	52.5	53.5	44.1	49.8	53.8	52.7	49.7
I	55.1	52.4	54.4	52.6	51.8	56.2	56.9	56.3	52.7	52.1	n/a	51.2	53.2	n/a	53.5	52.6	55.8	53.3
D	51.7	46.8	46.7	45.3	45.5	50.2	48.2	48.6	47.6	47.7	49.6	46.4	49.2	46.1	47.3	47.7	52.3	40.5
C	54.6	48.6	51.2	50.3	51.6	56.3	49.4	53.3	47.8	48.0	n/a	44.8	57.2	48.2	52.9	52.9	52.6	49.4
B	62.4	59.1	56.1	54.6	58.9	60.5	56.7	61.3	59.3	59.9	58.5	58.9	61.0	57.1	58.6	58.2	61.4	56.0
A	60.3	56.1	53.0	53.0	55.0	56.3	53.0	56.8	56.9	56.3	n/a	55.1	57.1	55.0	54.8	58.4	60.3	50.0
Loop	53.1	45.6	42.5	43.4	41.8	44.7	43.7	46.1	56.2	47.1	43.6	42.3	45.5	37.8	46.2	46.3	44.5	36.1

Table 6. Average Monthly Friction Measurements Using the Locked-Wheel Device at 80 kph (50 mph)

Section	Date																
	Feb 07	Mar 07	Aug 07	Sep 07	Nov 07	Dec 07	Feb 08	Dec 06	Jan 07	Apr 07	May 07	Jun 07	Jul 07	Oct 07	Feb 08	Mar 08	Apr 08	Jun 08
Eastbound 80 kph (50 mph) Analog Equipment								**Eastbound 80 kph (50 mph) Digital Equipment**										
Loop	50.4	52.5	46.9	53.1	46.2	49.5	50.4	47.4	53.4	49.4	52.7	50.2	55.4	45.7	46.3	47.5	49.5	44.8
A	39.0	38.6	38.5	41.4	32.7	40.6	37.0	37.2	36.6	33.1	n/a	32.8	38.0	32.3	32.7	40.5	33.5	35.0
B	43.8	44.9	42.5	40.6	37.3	40.4	40.4	37.7	39.9	31.9	42.5	30.3	39.2	30.7	36.5	43.3	38.8	39.5
C	44.6	40.5	38.6	41.5	34.6	41.2	38.4	38.8	39.7	37.4	n/a	36.4	42.0	31.3	36.8	38.7	39.7	39.1
D	31.5	30.5	29.5	33.3	28.1	30.4	31.2	31.7	30.4	29.8	42.3	23.9	28.1	24.7	30.6	32.0	32.3	31.7
I	52.0	50.5	49.6	47.2	46.9	48.1	47.1	46.8	48.4	46.7	n/a	44.4	47.7	n/a	48.3	50.5	52.2	45.6
J	55.2	51.6	51.9	51.7	43.2	51.5	49.7	50.0	50.5	49.4	50.3	49.2	51.3	44.3	50.4	48.7	50.4	43.0
K	39.7	39.9	45.8	47.6	45.0	46.1	45.6	34.5	37.4	41.8	n/a	42.9	46.5	45.9	43.1	43.8	48.4	43.1
L	46.1	45.8	44.7	44.2	40.7	44.1	42.2	43.2	45.7	44.1	49.9	40.7	43.7	40.4	40.7	40.4	43.6	35.9
Westbound 80 kph (50 mph) Analog Equipment								**Westbound 80 kph (50 mph) Digital Equipment**										
L	48.7	49.1	43.7	45.2	39.2	45.4	43.9	47.0	42.8	48.2	49.2	42.4	45.3	41.9	43.4	44.2	48.9	40.0
K	41.4	44.1	48.5	47.0	46.4	45.9	44.8	38.5	37.8	44.9	n/a	41.9	48.2	45.3	45.7	43.1	50.8	42.9
J	49.2	50.4	47.5	48.3	37.9	49.7	43.6	43.1	42.7	45.7	47.6	44.0	43.7	47.5	42.4	47.7	51.2	45.2
I	50.6	45.8	42.9	47.4	37.3	45.2	45.3	47.4	47.2	47.2	n/a	43.0	43.9	n/a	46.0	46.9	46.3	45.7
D	46.2	47.1	40.5	39.9	34.3	42.3	40.8	39.1	44.9	41.6	44.3	36.6	42.2	35.4	38.2	39.3	38.8	34.4
C	48.4	48.9	44.9	42.9	38.9	45.5	43.9	43.9	43.8	45.3	n/a	36.5	46.3	38.0	44.2	48.1	44.9	40.4
B	55.5	53.3	53.3	51.7	49.8	53.4	52.4	52.0	52.5	54.4	54.8	53.1	52.4	44.5	48.9	49.7	50.8	46.4
A	55.1	52.9	50.0	50.7	47.0	50.1	48.5	49.4	54.8	51.1	n/a	45.6	50.7	46.3	46.9	51.9	47.2	43.3
Loop	37.0	37.4	37.6	34.9	33.1	42.2	37.3	37.7	n/a	40.0	46.4	33.9	35.4	29.1	53.0	34.5	36.4	34.7

Table 7. Averages and Standard Deviations by Device

Section	Eastbound				Westboundl			
	Analog		Digital		Analog		Digital	
	Total Average	Std Dev	Total Average	Std Dev	Total Average	Std Dev	Total Average	Std Dev
32 kph (20 mph)								
Loop	77.18	1.91	78.17	3.51	73.17	3.25	71.14	3.71
A	76.84	2.46	77.61	1.14	78.97	2.79	78.43	3.71
B	78.38	2.68	78.78	3.03	80.66	2.40	80.70	3.59
C	75.05	2.35	76.43	2.03	77.56	2.22	77.60	2.74
D	66.98	3.20	69.68	3.47	74.03	3.01	74.27	3.07
I	77.06	1.28	77.62	3.01	78.76	1.47	79.56	2.12
J	77.87	1.52	75.99	5.57	75.16	4.51	74.38	6.01
K	62.37	3.02	63.00	4.31	61.58	2.49	61.18	4.28
L	69.33	2.93	68.88	2.39	68.91	3.14	68.04	3.65
64 kph (40 mph)								
Loop	56.72	3.61	57.68	2.28	44.98	3.80	45.67	4.90
A	44.36	2.52	45.93	3.03	55.24	2.66	56.28	1.27
B	46.65	2.93	48.08	4.15	58.33	2.70	59.19	1.34
C	48.82	2.43	47.68	3.32	51.72	2.78	50.65	4.07
D	36.73	2.96	38.76	3.10	47.77	2.39	47.78	1.17
I	54.09	3.44	54.76	1.92	54.18	1.99	53.09	1.60
J	57.76	1.81	55.79	4.06	49.64	3.06	50.22	3.56
K	49.89	3.01	46.96	5.34	49.73	3.84	47.08	4.04
L	49.92	1.52	49.51	1.51	50.46	1.94	50.12	2.82
80 kph (50 mph)								
Loop	49.85	2.61	49.78	3.39	37.08	2.79	38.75	7.64
A	38.26	2.85	35.39	3.08	50.62	2.71	49.58	3.16
B	41.41	2.56	36.88	4.94	52.76	1.74	51.36	3.21
C	39.91	3.12	37.65	3.11	44.78	3.40	43.27	3.98
D	30.65	1.65	29.27	3.09	41.58	4.28	40.17	3.29
I	48.77	1.99	47.54	1.90	44.93	4.11	45.94	1.78
J	50.67	3.69	49.34	2.03	46.67	4.46	44.92	2.20
K	44.25	3.12	41.98	4.11	45.45	2.28	43.18	3.60
L	44.00	1.92	42.87	2.44	45.03	3.33	44.93	2.63

`

Table 8. Average Monthly Friction Measurements Using the DFTester at 20 kph (12.4 mph)

Section	Date												
	May 07	**Jun 07**	**Jul 07**	**Aug 07**	**Sep 07**	**Oct 07**	**Nov 07**	**Dec 07**	**Jan 08**	**Apr 08**	**May 08**	**Jun 08**	**Jul 08**
Eastbound DFTester 20 kph (12.4 mph)													
Loop	0.79	0.78	0.80	0.77	0.78	0.81	0.85	0.83	0.85	0.84	0.81	0.81	0.80
A	0.84	0.81	0.83	0.80	0.83	0.88	0.93	0.91	0.92	0.89	0.87	0.87	0.88
B	0.85	0.82	0.85	0.83	0.84	0.88	0.90	0.91	0.94	0.91	0.88	0.89	0.91
C	0.83	0.79	0.82	0.78	0.80	0.84	0.88	0.86	0.89	0.84	0.83	0.83	0.85
D	0.81	0.79	0.80	0.78	0.79	0.84	0.87	0.86	0.88	0.85	0.80	0.85	0.86
I	0.84	0.82	0.81	0.81	0.80	0.86	0.87	0.86	0.89	0.85	0.83	0.85	0.88
J	0.82	0.80	0.81	0.73	0.75	0.81	0.82	0.83	0.82	0.85	0.75	0.83	0.86
K	0.63	0.65	0.66	0.66	0.69	0.67	0.70	0.71	0.73	0.68	0.65	0.65	0.69
L	0.73	0.72	0.74	0.74	0.77	0.73	0.77	0.79	0.79	0.75	0.74	0.74	0.76
Westbound DFTester 20 kph (12.4 mph)													
L	0.76	0.73	0.73	0.72	0.72	0.74	0.78	0.79	0.81	0.76	0.72	0.73	0.77
K	0.64	0.63	0.66	0.66	0.65	0.67	0.67	0.71	0.72	0.67	0.64	0.68	0.68
J	0.80	0.79	0.75	0.75	0.78	0.82	0.84	0.84	0.85	0.82	0.77	0.80	0.80
I	0.85	0.82	0.80	0.79	0.81	0.85	0.87	0.85	0.89	0.86	0.80	0.75	0.84
D	0.79	0.78	0.77	0.77	0.79	0.83	0.86	0.85	0.90	0.85	0.82	0.81	0.82
C	0.80	0.79	0.78	0.77	0.80	0.82	0.84	0.85	0.87	0.83	0.79	0.82	0.81
B	0.81	0.80	0.79	0.80	0.82	0.82	0.85	0.84	0.86	0.85	0.79	0.84	0.82
A	0.85	0.81	0.80	0.82	0.82	0.86	0.86	0.87	0.88	0.89	0.81	0.84	0.83
Loop	0.78	0.77	0.78	0.75	0.81	0.84	0.84	0.84	0.85	0.78	0.80	0.77	0.82

Table 9. Average Monthly Friction Measurements Using the DFTester at 32 kph (20 mph)

Section	Date												
	May 07	**Jun 07**	**Jul 07**	**Aug 07**	**Sep 07**	**Oct 07**	**Nov 07**	**Dec 07**	**Jan 08**	**Apr 08**	**May 08**	**Jun 08**	**Jul 08**
Eastbound DFTester 32 kph (20 mph)													
Loop	0.76	0.76	0.78	0.75	0.76	0.79	0.82	0.80	0.82	0.81	0.78	0.78	0.77
A	0.82	0.80	0.82	0.79	0.82	0.86	0.90	0.89	0.89	0.86	0.85	0.85	0.86
B	0.84	0.81	0.84	0.82	0.83	0.86	0.88	0.89	0.93	0.88	0.86	0.86	0.89
C	0.81	0.78	0.81	0.77	0.79	0.83	0.85	0.84	0.86	0.82	0.82	0.81	0.82
D	0.79	0.78	0.79	0.77	0.77	0.81	0.84	0.84	0.84	0.82	0.78	0.82	0.83
I	0.82	0.81	0.80	0.80	0.79	0.84	0.85	0.84	0.87	0.83	0.81	0.82	0.86
J	0.80	0.79	0.80	0.72	0.73	0.79	0.80	0.80	0.80	0.82	0.74	0.81	0.84
K	0.60	0.61	0.64	0.63	0.65	0.63	0.69	0.67	0.69	0.64	0.62	0.62	0.65
L	0.71	0.70	0.73	0.72	0.75	0.72	0.75	0.75	0.76	0.73	0.72	0.72	0.72
Westbound DFTester 32 kph (20 mph)													
L	0.74	0.71	0.71	0.71	0.70	0.73	0.75	0.76	0.78	0.74	0.71	0.71	0.74
K	0.60	0.60	0.63	0.64	0.62	0.63	0.64	0.66	0.67	0.64	0.62	0.64	0.65
J	0.79	0.77	0.75	0.75	0.77	0.80	0.82	0.82	0.83	0.80	0.75	0.77	0.78
I	0.82	0.81	0.80	0.78	0.80	0.83	0.84	0.83	0.86	0.84	0.79	0.72	0.82
D	0.77	0.77	0.75	0.76	0.77	0.81	0.83	0.83	0.85	0.83	0.80	0.78	0.79
C	0.79	0.78	0.78	0.76	0.79	0.81	0.82	0.83	0.85	0.81	0.77	0.79	0.79
B	0.80	0.79	0.78	0.79	0.80	0.80	0.84	0.82	0.84	0.83	0.78	0.81	0.80
A	0.83	0.79	0.79	0.81	0.81	0.84	0.84	0.85	0.87	0.87	0.80	0.82	0.80
Loop	0.74	0.74	0.76	0.73	0.78	0.80	0.80	0.81	0.81	0.75	0.77	0.73	0.78

Table 10. Average Monthly Friction Measurements Using the DFTester at 64 kph (40 mph)

Section	Date												
	May 07	**Jun 07**	**Jul 07**	**Aug 07**	**Sep 07**	**Oct 07**	**Nov 07**	**Dec 07**	**Jan 08**	**Apr 08**	**May 08**	**Jun 08**	**Jul 08**
Eastbound DFTester 64 kph (40 mph)													
Loop	0.69	0.70	0.72	0.69	0.70	0.71	0.73	0.72	0.73	0.72	0.71	0.69	0.69
A	0.76	0.76	0.78	0.75	0.76	0.79	0.81	0.82	0.80	0.78	0.78	0.76	0.77
B	0.77	0.77	0.79	0.77	0.77	0.79	0.80	0.80	0.82	0.80	0.80	0.78	0.80
C	0.75	0.74	0.76	0.73	0.73	0.75	0.77	0.76	0.77	0.75	0.76	0.72	0.74
D	0.73	0.74	0.75	0.73	0.72	0.74	0.74	0.75	0.75	0.74	0.73	0.73	0.74
I	0.76	0.76	0.76	0.76	0.74	0.77	0.77	0.77	0.79	0.76	0.76	0.74	0.77
J	0.74	0.74	0.75	0.68	0.67	0.72	0.71	0.72	0.71	0.76	0.68	0.73	0.76
K	0.53	0.55	0.57	0.57	0.57	0.54	0.62	0.58	0.59	0.59	0.56	0.55	0.58
L	0.65	0.65	0.67	0.66	0.68	0.66	0.68	0.65	0.65	0.67	0.65	0.65	0.63
Westbound DFTester 64 kph (40 mph)													
L	0.68	0.66	0.66	0.66	0.65	0.68	0.69	0.67	0.69	0.66	0.66	0.65	0.66
K	0.54	0.55	0.57	0.57	0.56	0.56	0.58	0.58	0.58	0.58	0.58	0.58	0.59
J	0.72	0.72	0.71	0.71	0.72	0.73	0.74	0.74	0.74	0.73	0.73	0.71	0.70
I	0.75	0.76	0.75	0.73	0.75	0.76	0.76	0.76	0.78	0.77	0.77	0.66	0.74
D	0.71	0.72	0.71	0.71	0.72	0.73	0.73	0.74	0.75	0.75	0.75	0.71	0.71
C	0.73	0.73	0.73	0.72	0.73	0.74	0.74	0.75	0.76	0.74	0.74	0.72	0.72
B	0.74	0.74	0.74	0.74	0.75	0.74	0.77	0.76	0.78	0.76	0.76	0.75	0.74
A	0.77	0.74	0.74	0.76	0.76	0.77	0.76	0.78	0.79	0.79	0.79	0.74	0.73
Loop	0.66	0.68	0.70	0.68	0.71	0.79	0.70	0.72	0.72	0.68	0.68	0.65	0.69

Table 11. Average Monthly Friction Measurements Using the DFTester at 80 kph (50 mph)

Section	Date												
	May 07	**Jun 07**	**Jul 07**	**Aug 07**	**Sep 07**	**Oct 07**	**Nov 07**	**Dec 07**	**Jan 08**	**Apr 08**	**May 08**	**Jun 08**	**Jul 08**
Eastbound DFTester 80 kph (50 mph)													
Loop	0.65	0.65	0.66	0.65	0.65	0.65	0.67	0.66	0.66	0.66	0.65	0.64	0.63
A	0.69	0.69	0.70	0.68	0.70	0.70	0.71	0.71	0.71	0.69	0.70	0.69	0.69
B	0.70	0.70	0.72	0.71	0.70	0.71	0.71	0.73	0.72	0.71	0.71	0.70	0.71
C	0.68	0.68	0.70	0.67	0.67	0.68	0.69	0.69	0.68	0.67	0.68	0.63	0.67
D	0.67	0.68	0.68	0.68	0.66	0.67	0.67	0.67	0.67	0.67	0.66	0.67	0.66
I	0.70	0.70	0.69	0.70	0.68	0.70	0.70	0.70	0.71	0.69	0.68	0.67	0.70
J	0.68	0.68	0.69	0.63	0.63	0.66	0.64	0.66	0.65	0.69	0.62	0.67	0.68
K	0.51	0.53	0.54	0.55	0.54	0.51	0.57	0.55	0.56	0.55	0.54	0.53	0.55
L	0.61	0.60	0.62	0.61	0.63	0.61	0.62	0.59	0.59	0.61	0.61	0.60	0.57
Westbound DFTester 80 kph (50 mph)													
L	0.63	0.62	0.62	0.61	0.61	0.62	0.63	0.61	0.63	0.61	0.62	0.61	0.60
K	0.53	0.54	0.53	0.55	0.54	0.54	0.55	0.54	0.54	0.56	0.56	0.56	0.55
J	0.67	0.66	0.66	0.65	0.67	0.67	0.67	0.68	0.67	0.65	0.66	0.65	0.65
I	0.70	0.70	0.69	0.67	0.69	0.68	0.68	0.68	0.70	0.70	0.67	0.66	0.66
D	0.66	0.67	0.66	0.67	0.67	0.67	0.66	0.67	0.68	0.68	0.68	0.65	0.65
C	0.67	0.68	0.68	0.67	0.67	0.68	0.67	0.68	0.69	0.67	0.67	0.66	0.66
B	0.79	0.75	0.70	0.77	0.81	0.82	0.83	0.71	0.70	0.70	0.68	0.68	0.68
A	0.82	0.75	0.69	0.77	0.82	0.81	0.80	0.71	0.71	0.71	0.67	0.68	0.67
Loop	0.74	0.71	0.65	0.74	0.85	0.82	0.81	0.66	0.65	0.62	0.64	0.60	0.63

4.2 Results

The friction results measured by the DFTester for all months are higher than those measured by the locked-wheel device. Figure 19 shows a comparison of friction values obtained in June 2008 on the same sections. These differences may have occurred because both devices operate differently.

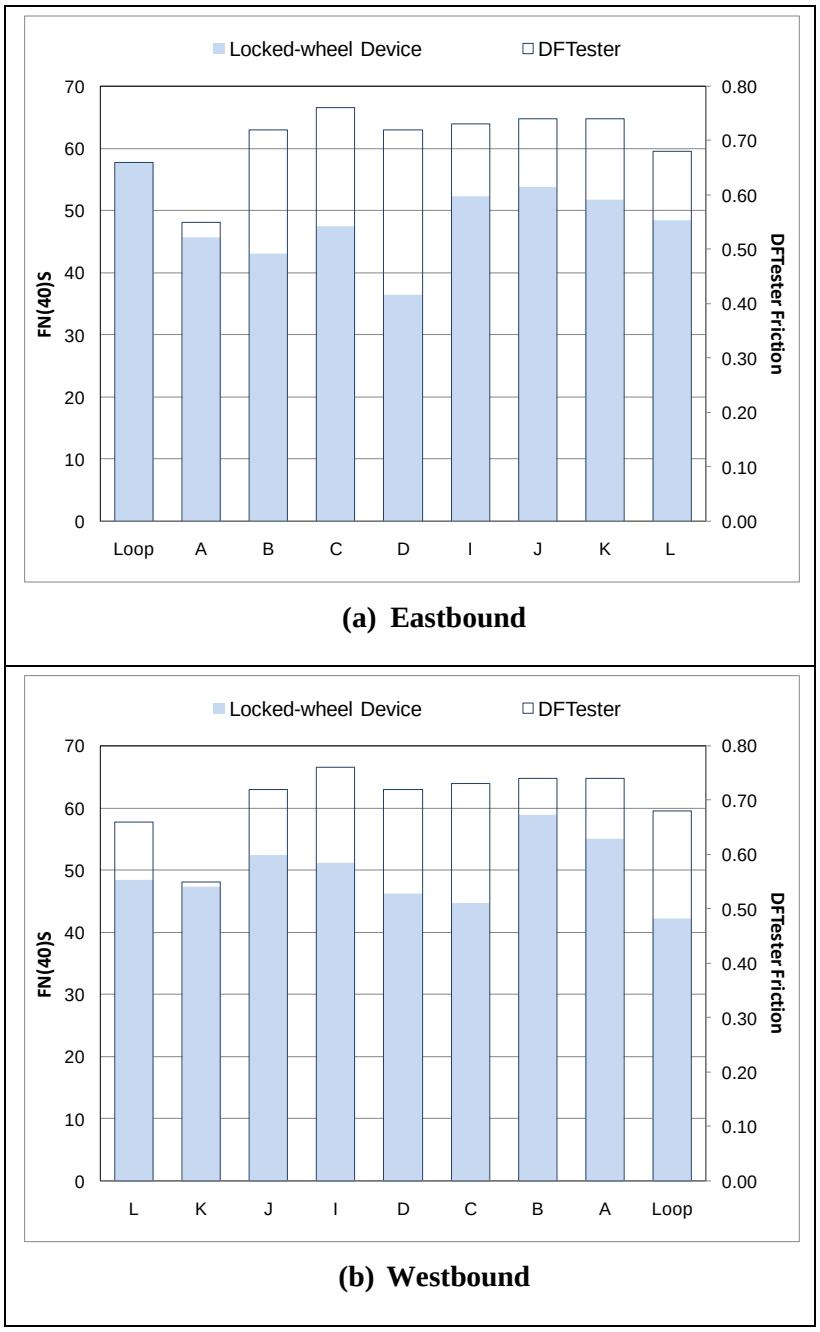

Figure 19. Friction Measurements Using the Locked-Wheel Device and the DFTester (on 06-25-08) Measured at 64 kph (40 mph)

4.3 Pavement Macrotexture Measurements

Texture measurements were collected the same months that friction was measured (December 2006 through June 2008). These tests were carried out on the same three locations used for the DFTester. The average of the three locations was calculated and reported as the texture value for each section and direction. Table 12 summarizes the average texture measurement values obtained.

4.4 DFTester-Skid Number Measurements Comparison

To compare friction measurements obtained by the DFTester with the ones obtained using the locked-wheel device for all months and sections at 32 kph (20 mph), the two measurements were plotted. A regression analysis was calculated (Figure 20). The coefficient of determination for the relationship between DFTester and locked-wheel device measurements (R^2) is 0.43, which shows a similar friction measurement tendency at this speed. However, at speeds of 64 kph (40 mph) and 80 kph (50 mph), no significant correlation was observed.

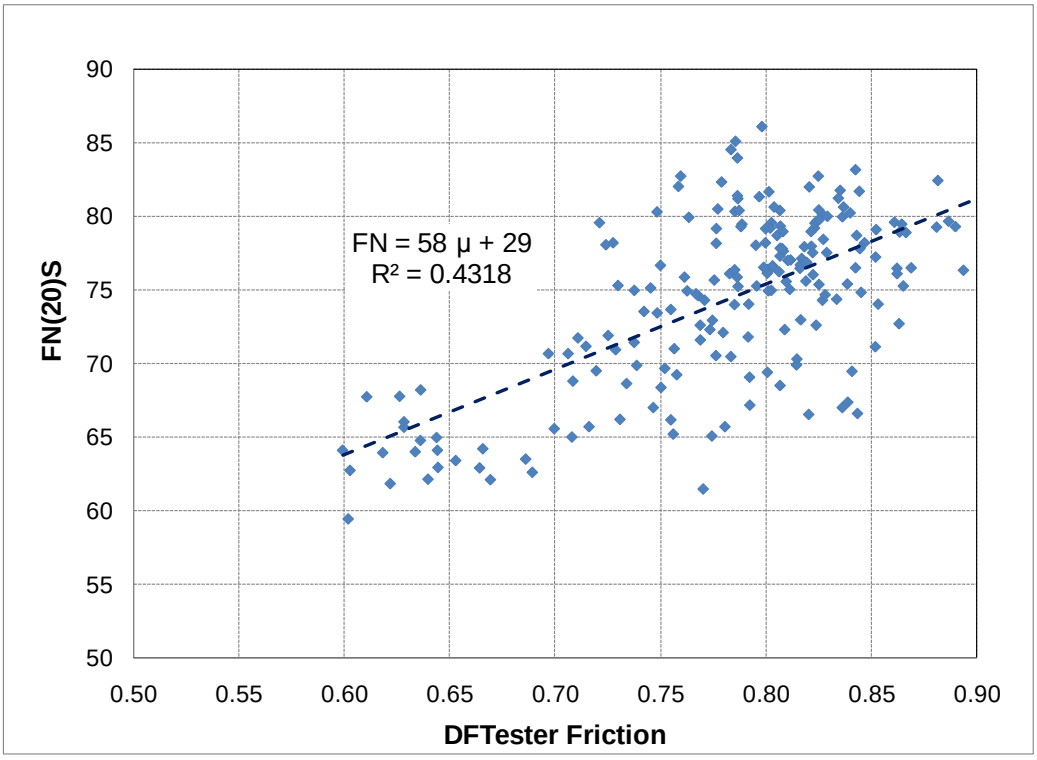

Figure 20. Correlation between DFTester and Locked-Wheel Device Measurements at 32 kph (20 mph)

Table 12. Average Texture Numbers Obtained Using the CTMeter

Section	Date																	
	Dec 06	**Feb 07**	**Mar 07**	**Apr 07**	**May 07**	**Jun 07**	**Jul 07**	**Aug 07**	**Sep 07**	**Oct 07**	**Nov 07**	**Dec 07**	**Jan 08**	**Feb 08**	**Mar 08**	**Apr 08**	**May 08**	**Jun 08**
	Eastbound																	
Loop	0.97	1.05	1.01	0.84	1.03	1.16	1.05	1.01	1.04	1.04	1.03	1.10	1.13	1.06	1.06	1.04	1.00	1.05
A	0.50	0.49	0.51	0.95	0.52	0.49	0.48	0.84	0.52	0.50	0.54	0.55	0.54	0.57	0.50	0.74	0.53	0.53
B	0.66	0.64	0.67	1.01	0.65	0.66	0.63	1.03	0.65	0.68	0.76	0.72	0.75	0.70	0.74	0.68	0.68	0.74
C	0.65	0.62	0.66	0.77	0.63	0.64	0.65	0.79	0.67	0.64	0.66	0.65	0.70	0.68	0.73	0.68	0.71	0.73
D	0.54	0.61	0.51	0.77	0.48	0.52	0.49	0.70	0.52	0.53	0.57	0.51	0.57	0.58	0.57	0.55	0.55	0.57
I	0.79	0.83	0.81	0.69	0.83	0.82	0.86	0.67	0.95	0.86	0.94	0.85	0.94	0.87	0.91	0.88	0.92	0.95
J	0.95	1.02	0.94	0.79	0.84	0.94	0.83	0.79	0.88	0.82	1.06	0.94	0.88	0.93	1.01	0.97	1.04	0.91
K	1.38	1.64	1.36	1.76	1.41	1.34	1.29	1.43	1.33	1.41	1.51	1.67	1.45	1.71	1.90	1.41	1.62	1.48
L	0.86	0.87	0.90	1.01	0.87	0.93	1.00	0.99	0.94	0.89	0.97	0.89	0.88	0.86	1.08	0.91	1.00	0.90
	Westbound																	
L	1.13	1.10	1.00	0.87	1.07	1.17	1.06	0.91	1.10	1.18	1.14	1.06	1.09	0.99	1.05	0.95	1.08	1.13
K	1.48	1.90	1.60	1.41	1.64	1.70	1.56	1.55	1.80	1.71	1.58	1.67	1.66	1.51	1.76	1.57	1.80	1.74
J	0.86	0.84	0.98	0.95	0.81	0.81	0.77	0.87	0.87	0.79	0.75	0.85	0.89	0.88	0.81	0.75	0.85	0.82
I	0.58	0.65	0.73	0.81	0.68	0.68	0.72	0.91	0.66	0.71	0.71	0.68	0.68	0.73	0.72	0.72	0.72	0.76
D	0.76	0.62	0.71	0.65	0.68	0.69	0.67	0.56	0.67	0.71	0.68	0.72	0.73	0.71	0.68	0.69	0.70	0.71
C	0.74	0.81	0.69	0.67	0.70	0.69	0.74	0.62	0.80	0.73	0.76	0.78	0.80	0.71	0.74	0.80	0.79	0.77
B	0.95	1.04	1.09	0.73	1.08	0.94	1.03	0.72	1.01	0.99	0.97	1.10	1.05	1.00	0.99	1.08	1.01	1.10
A	0.83	0.80	0.82	0.52	0.94	0.92	0.88	0.53	0.90	0.88	0.87	0.94	0.86	0.85	0.85	0.71	0.89	0.92
Loop	0.85	0.99	1.03	0.98	0.79	0.91	0.75	0.78	0.85	0.89	0.78	0.88	0.97	0.87	0.90	0.91	0.80	0.85

CHAPTER 5. DATA ANALYSIS

To analyze the effect of seasonal variation on pavement friction properties, monthly friction correction factors were computed for each pavement section and speed. Sinusoidal models were fitted to the average friction correction factors to predict the average monthly seasonal friction variation at various speeds. Finally the effect of macrotexture on the friction correction factors was also investigated.

5.1 Calculation of Friction Correction Factors

In order to compare friction measurements taken on different sections, the monthly friction values were normalized by dividing the value obtained each month by the August 2007 values. Measurements during this month are theoretically the lowest friction numbers observed throughout the analyzed period because that is the month with the highest recorded temperature in such period. The resulting numbers can be considered friction correction factors to bring the friction measurements to the lowest value. These correction factors are used in various DOTs.

In order to observe the monthly variation of friction for all sections, these factors are plotted for all speeds against time in Figures 21 and 22, for the DFTester and the locked-wheel device, respectively. The charts also display the average friction correction factor for all sections as a solid line. The plots show that the seasonal (or monthly) changes are different for the various sections. In general, the plots show that the lowest correction factors correspond to the hottest month of the period year, August. This justifies the initial assumption of dividing all monthly friction values (December 2006 through July 2008) by the friction value measured in August.

However, there are several sections, such as K, L, and Loop, measured with both devices that have many correction factors less than 1. This may be explained by the fact that the three sections have different surface mix materials: K is an OGFC, and L and Loop are SMA mixes. In addition, there are also other inconsistencies.

A comparison of the two figures shows that the friction correction factors for the DFTester appear to follow a more cyclical trend than those for the locked-wheel device. It is also clear that seasonal effect can explain only a small portion of the variability observed in the measurements.

Table 13 compares the average locked-wheel device results with the correction factors used by VDOT for measurements collected at 64 kph (40 mph). Current VDOT factors (NHCRP, 2000) are significantly higher than those obtained at the Smart Road. However, they follow a similar cyclical trend.

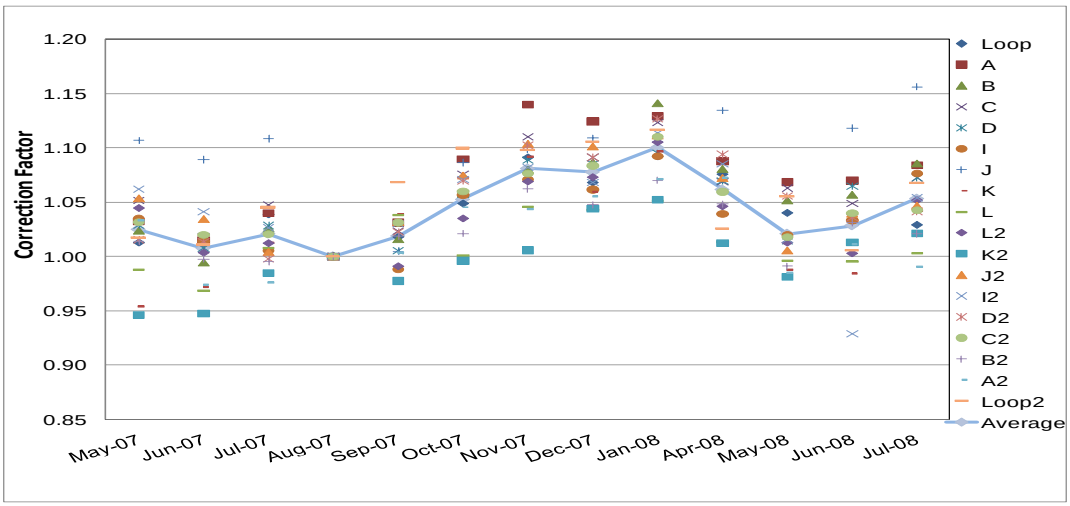

(a) 32 kph (20 mph)

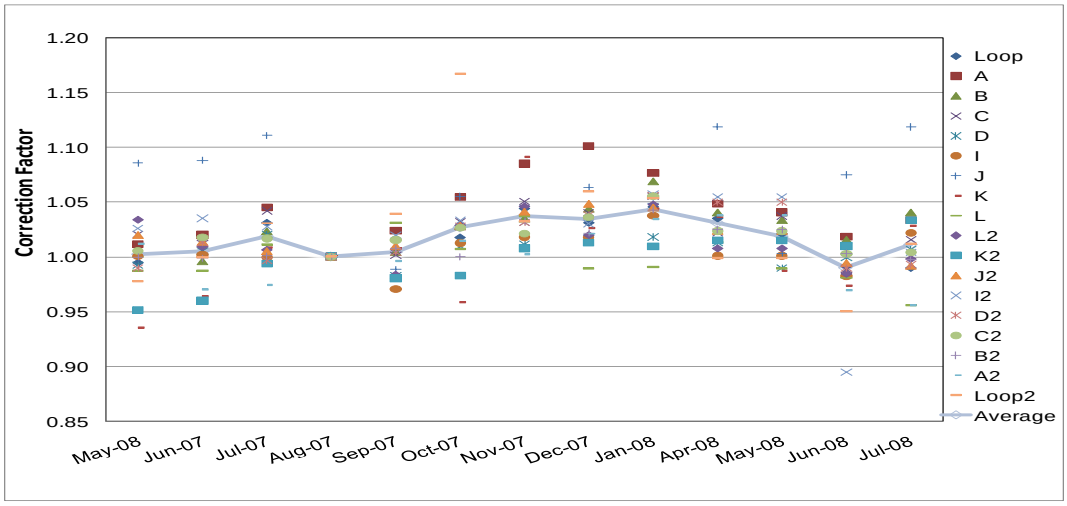

(b) 64 kph (40 mph)

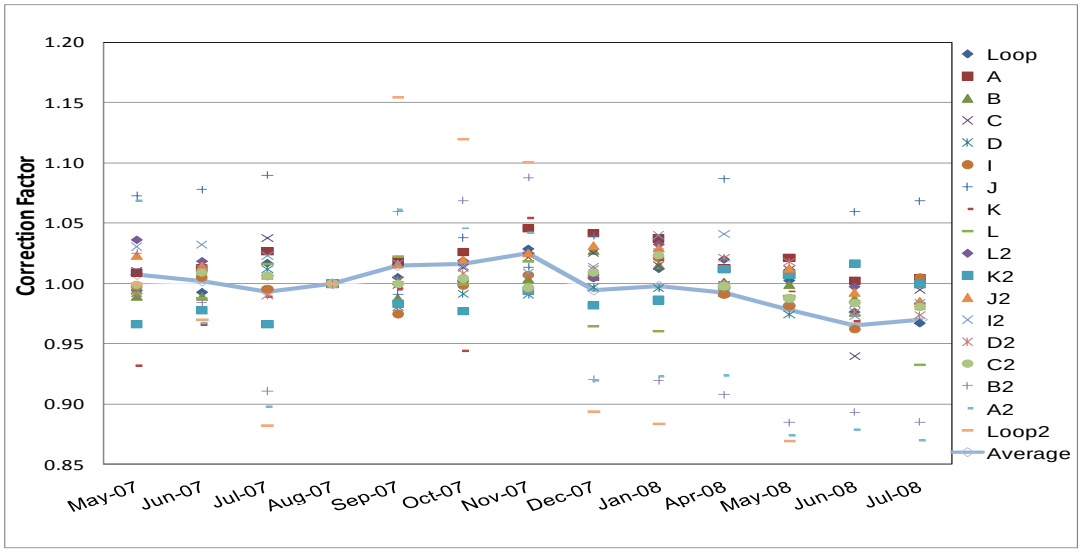

(c) 80 kph (50 mph)

Figure 21. Measured DFTester Friction Correction Factors

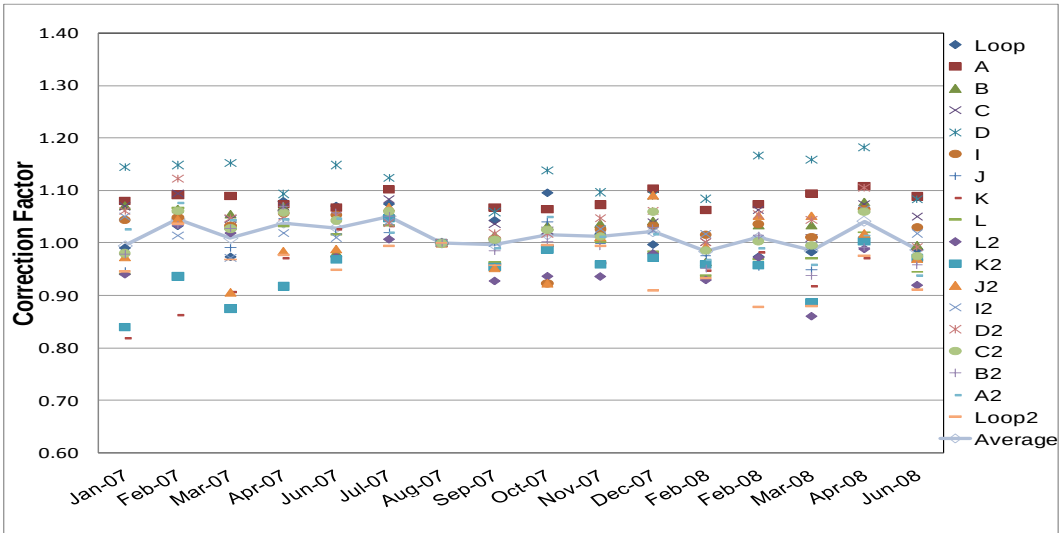

(a) 32 kph (20 mph)

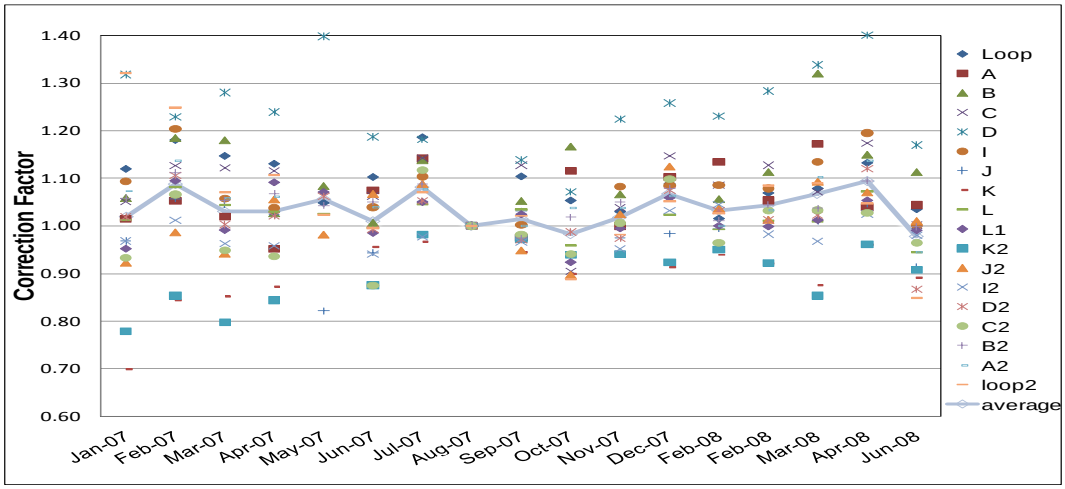

(b) 64 kph (40 mph)

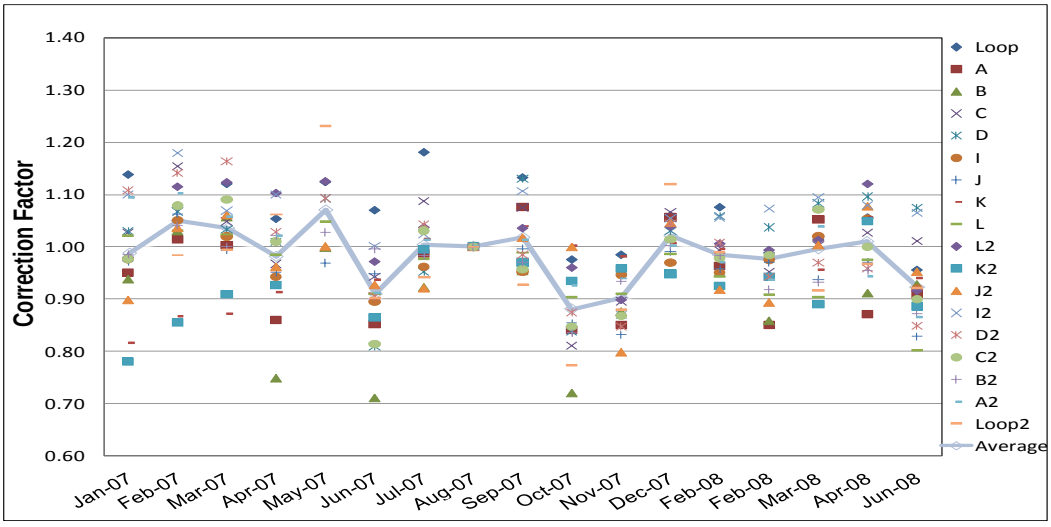

(c) 80 kph (50 mph)

Figure 22. Measured Locked-Wheel Device Friction Correction Factors

Table 13. Comparison of Friction Correction Factors

Friction Correction Factor	Month											
	May	**Jun**	**July**	**Aug**	**Sep**	**Oct**	**Nov**	**Dec**	**Jan**	**Feb**	**Mar**	**Apr**
Average	1.05	1.03	1.01	1.00	1.00	1.01	1.03	1.06	1.07	1.08	1.07	1.07
Current VDOT	1.09	1.02	1.00	1.00	1.04	1.11	1.15	1.16	1.16	1.15	1.15	1.14

5.2 Friction Correction Factor Models

After studying the friction variation throughout the year, a sinusoidal model fit was chosen to predict the friction correction factors for every month and speed (Equation 5.1).

$$CF = 1 + \alpha(1 - \sin((M - \beta) \times \frac{\pi}{6}) \quad (5.1)$$

Where:

CF = correction factor,

M = the number month of the year (e.g., January = 1), and

α and β= regression factors.

Best-fit models were developed for the locked-wheel device and DFTester measurements. The models were obtained by minimizing the mean squared error using the solver function of Excel. The model parameters obtained for the two friction measuring devices at three speeds are summarized in Table 14. The regression factor α represents the amplitude of the correction, and β the horizontal position. The standard error was calculated as the mean squared error of the residuals and is presented in the last row of Table 14.

Table 14. Model Parameters

Device	DFTester				Locked-Wheel Device		
Speed	**20 kph (12.4 mph)**	**32 kph (20 mph)**	**64 kph (40 mph)**	**81 kph (50 mph)**	**32 kph (20 mph)**	**64 kph (40 mph)**	**81 kph (50 mph)**
α	-0.0584	-0.0502	-0.0223	-0.0043	-0.0170	-0.0420	-0.0192
β	16.287	16.240	16.105	14.477	5.824	17.344	6.007
Std Error	0.020	0.017	0.009	0.014	0.010	0.017	0.058

5.3 Friction Correction Factor Model for the DFTester

The average measured and predicted friction correction factors considering all the dense graded surface mixes for the DFTester is summarized in Table 15. The table also presents the average Temperature for the month.

Table 15. Average Monthly Friction Correction Factors for Measurements Taken with the DFTester on Dense Graded Mixes

Date		May	Jun	July	Aug	Sep	Oct	Nov	Dec	Jan	Feb	Mar	Apr	May	Jun	July
Temp (°F)		**62**	**69**	**70**	**76**	**67**	**59**	**43**	**39**	**32**	**38**	**44**	**52**	**59**	**70**	**69**
20 kph (12.4 mph)	Meas.	1.03	1.01	1.02	1.00	1.02	1.06	1.09	1.09	1.12	n/a	n/a	1.07	1.02	1.04	1.07
	Model	1.04	1.01	1.00	1.00	1.02	1.05	1.08	1.10	1.12	1.11	1.09	1.07	1.04	1.01	1.00
31 kph (20 mph)	Meas.	1.02	1.01	1.02	1.00	1.02	1.05	1.08	1.08	1.10	n/a	n/a	1.06	1.02	1.03	1.05
	Model	1.03	1.01	1.00	1.00	1.02	1.04	1.07	1.09	1.10	1.10	1.08	1.06	1.03	1.01	1.00
64 kph (40 mph)	Meas.	1.00	1.01	1.02	1.00	1.00	1.03	1.04	1.03	1.04	n/a	n/a	1.03	1.02	0.99	1.01
	Model	1.01	1.00	1.00	1.00	1.01	1.02	1.03	1.04	1.04	1.04	1.03	1.02	1.01	1.00	1.00
80.5 kph (50 mph)	Meas.	1.01	1.00	0.99	1.00	1.01	1.02	1.03	0.99	1.00	n/a	n/a	0.99	0.98	0.97	0.97
	Model	1.00	1.00	1.00	1.00	1.01	1.01	1.01	1.01	1.01	1.01	1.00	1.00	1.00	1.00	1.00

Figure 23 presents the fitted sinusoidal model for the data collected using the DFTester. The plot shows a very good agreement between the measured and predicted friction correction factors at 20 kph (12.4 mph). In addition these, results suggest that friction varies between 1.0 and 1.12 and that friction increases during winter months and decreases in the summer. The lowest friction correction factor occurs in the hottest months of the year, July and August.

Figure 24 shows the best fitted sinusoidal model for the friction correction factors for measurements at 32 kph (20 mph). The trend is very similar to the one observed at 20 kph (12.4 mph). It

is also observed that friction correction factors decrease with speed. The peak friction value for the coldest month of the year is slightly lower than the one predicted at 20 kph (12.4 mph).

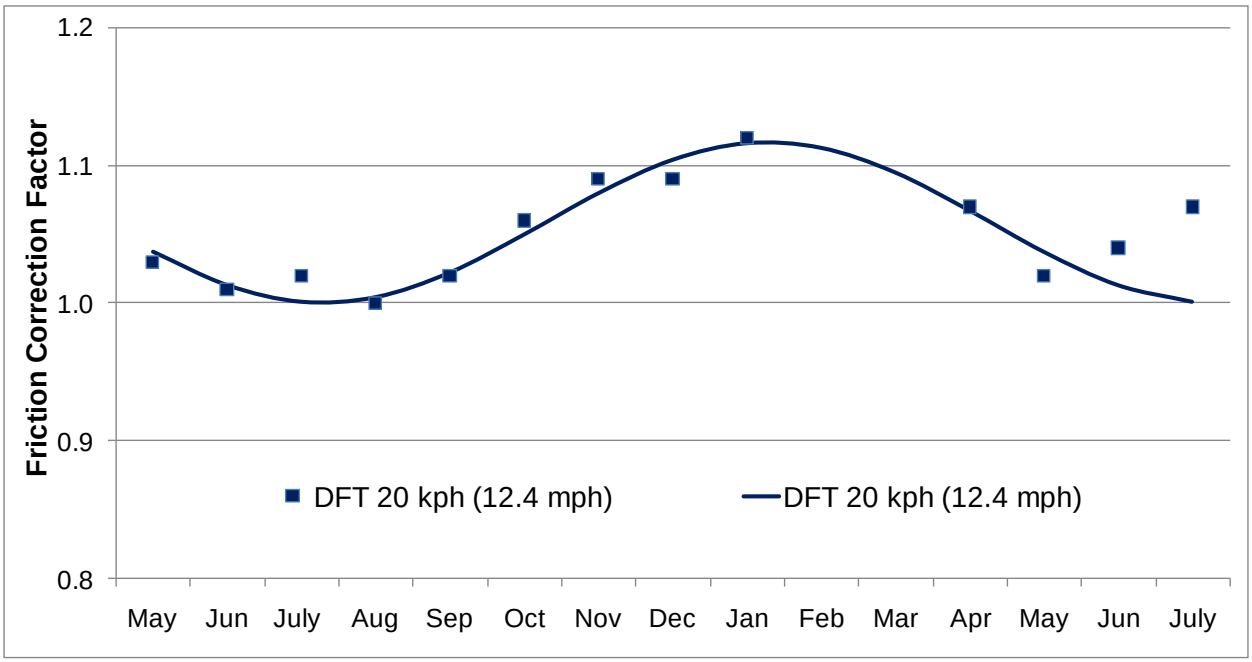

Figure 23. Predicted and Average Measured Friction Correction Factors for the DFTester Measurements at 20 kph (12.4 mph)

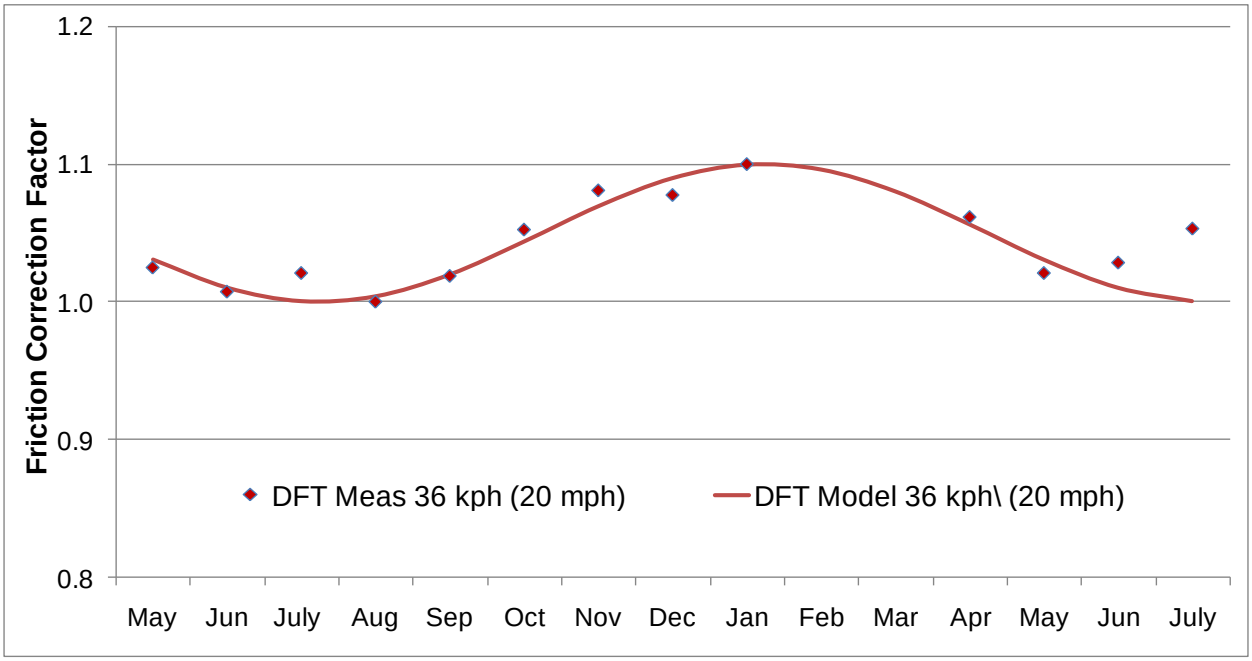

Figure 24. Predicted and Average Measured Friction Correction Factors for the DFTester Measurements at 32 kph (20 mph)

The best-fit sinusoidal model for the friction correction factors for measurements at 64 kph (40 mph) using the DFTester also fit the average measured factors well, as shown in Figure 25. The trend is similar to the one observed at 20 kph (12.4 mph).

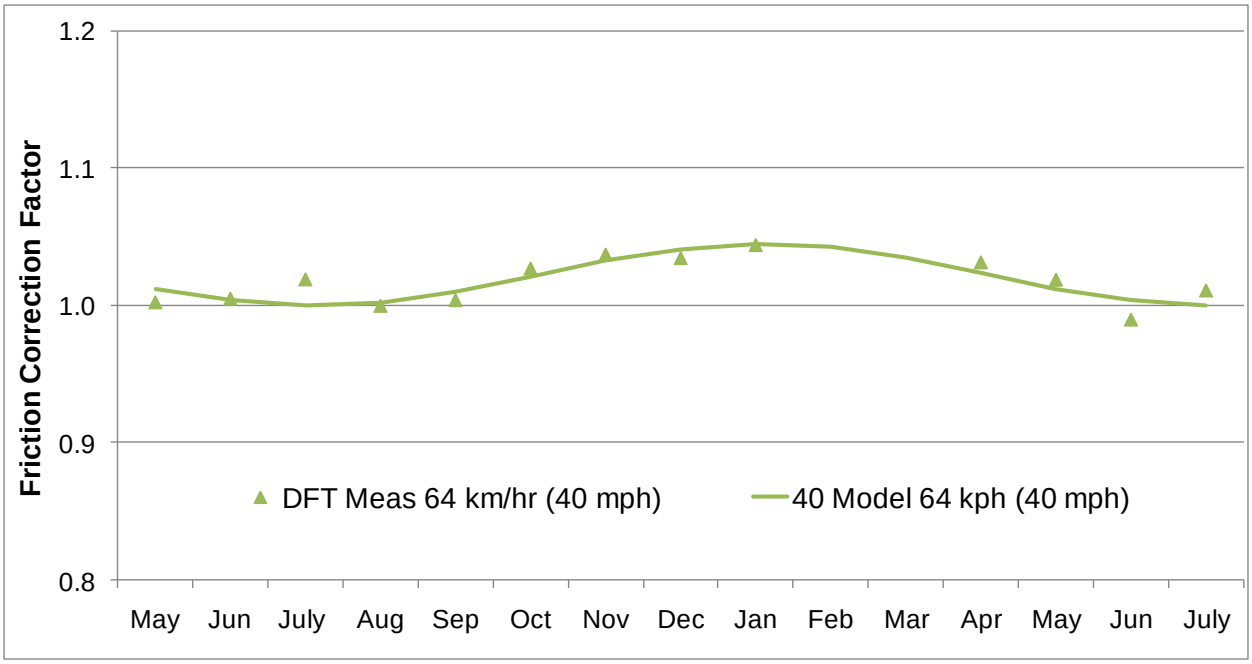

Figure 25. Predicted and Average Measured Friction Correction Factors for the DFTester Measurements at 64 kph (40 mph)

Figure 26 presents the best fitted model developed for the friction correction factors for measurements using the DFtester at 80 kph (50 mph). The figure suggests that the measurements at this speed do not follow a similar tendency to the observed trend at the other speeds. According to the initial assumption of normalizing all monthly friction values by dividing the value obtained each month by the August 2007 values, friction factors should be greater than 1 for all months. Another observation is that the friction variation is relatively small (between 0.97 and 1.01) and the fitted model has a greater standard error (0.014), which is in the same order of the magnitude as the overall variation.

Figure 27 compares the models for the measurements at the four speeds investigated. The figure shows that the cyclical pattern is consistent for the measurements at 20, 32, and 64 kph (12.4, 20, and 40 mph) and that the impact of the seasonal factors decreases with speed.

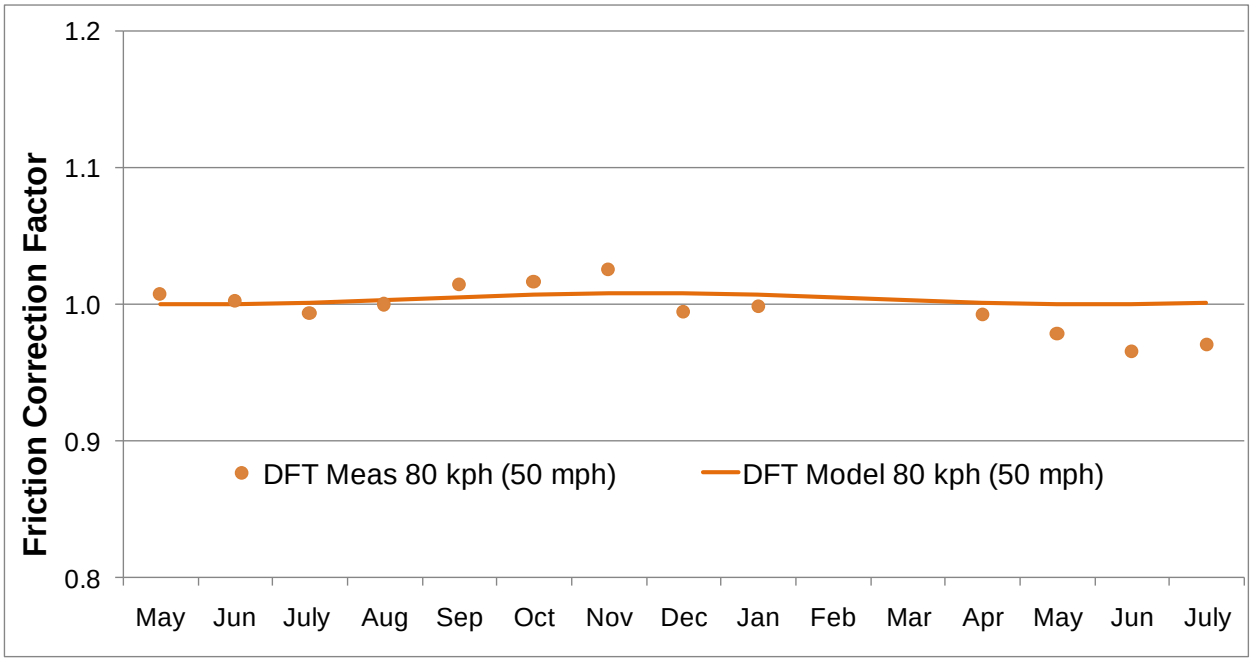

Figure 26. Predicted and Average Measured Friction Correction Factors for the DFTester Measurements at 81 kph (50 mph)

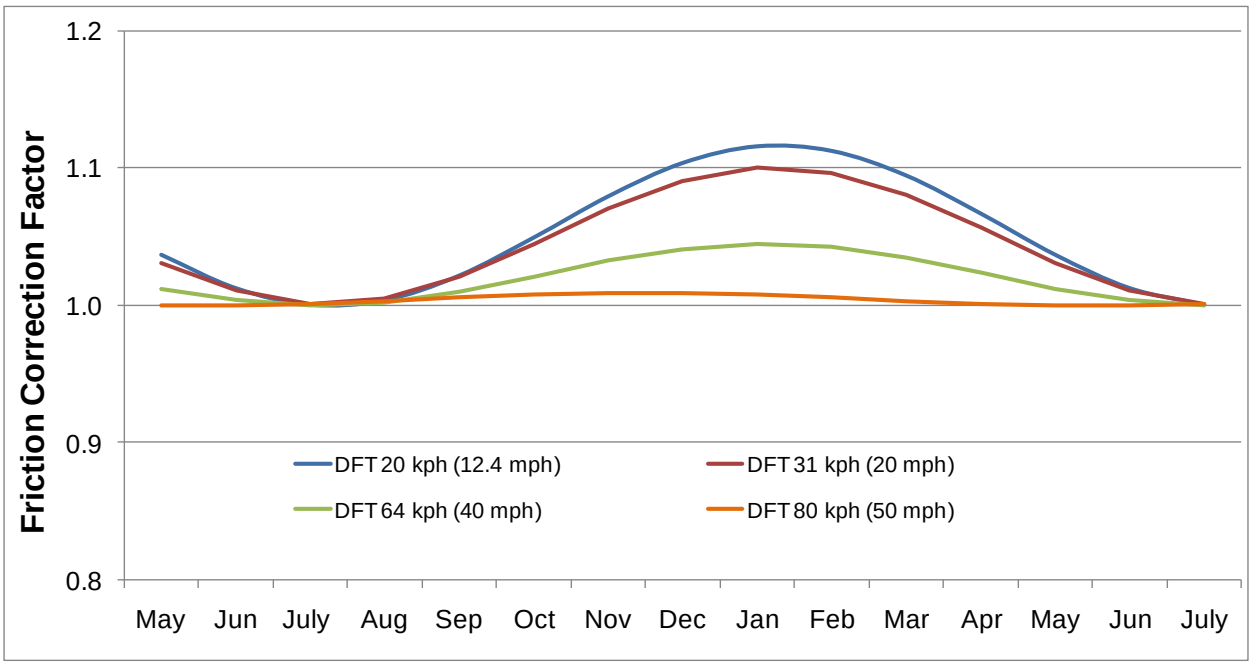

Figure 27. Comparison of the Developed Friction Corrections Factor Models for the DFTester Measurements at Different Speeds

The fitted sinusoidal model for speeds at 20, 32, and 64 kph (12.4, 20, and 40 mph) confirms that the peak friction value occurs during the coldest month of the year in Blacksburg. Figure 28 shows the average temperature for the tested months in Blacksburg according to the National Climate Data Center and compares the trend with the predicted correction factors at all DFTester speeds. This plot suggests that the hottest months of the year, July and August, coincide with the lowest friction values and the coldest month, January, with the highest friction values. This supports the assumption that temperature is an important factor to consider for seasonal friction variation.

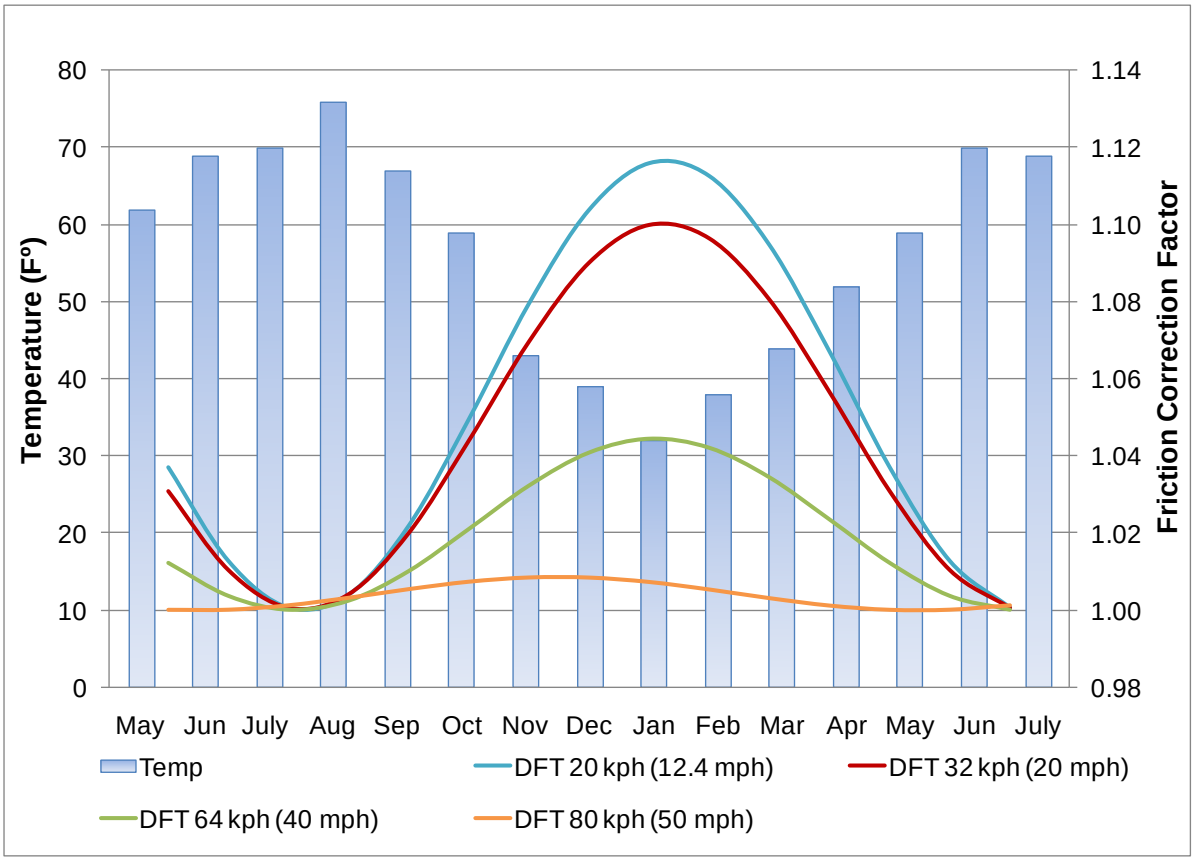

Figure 28. DFTester Friction Correction Factors and Average Monthly Temperatures in Blacksburg, May 2007 through July 2008

The sinusoidal model fitted to the friction measurements using the DFTester suggests that speed is an important parameter on the influence of seasonal friction variation. This effect was studied by making the parameter α dependent on speed. A good correlation ($R^2 = 0.996$) from a regression analysis was found (Figure 29). The relation is shown in Equation 5.2:

$$\alpha = -0.0009 \times (V) + 0.0074 \quad (5.2)$$

α = parameter depending on speed, and

V = Speed (kph).

The fitted sinusoidal equation was then modified to include speed (Equation 5.3):

$$CF = 1 + [(-0.009x(V) + 0.0074)(1 - \sin\left((M - 16.2) \times \frac{\pi}{6}\right))] \quad (5.3)$$

Where:

CF = correction factor,

V = Speed (kph),

M = the number month of the year (e.g., January = 1), and

β = 16.2 (adjusted number).

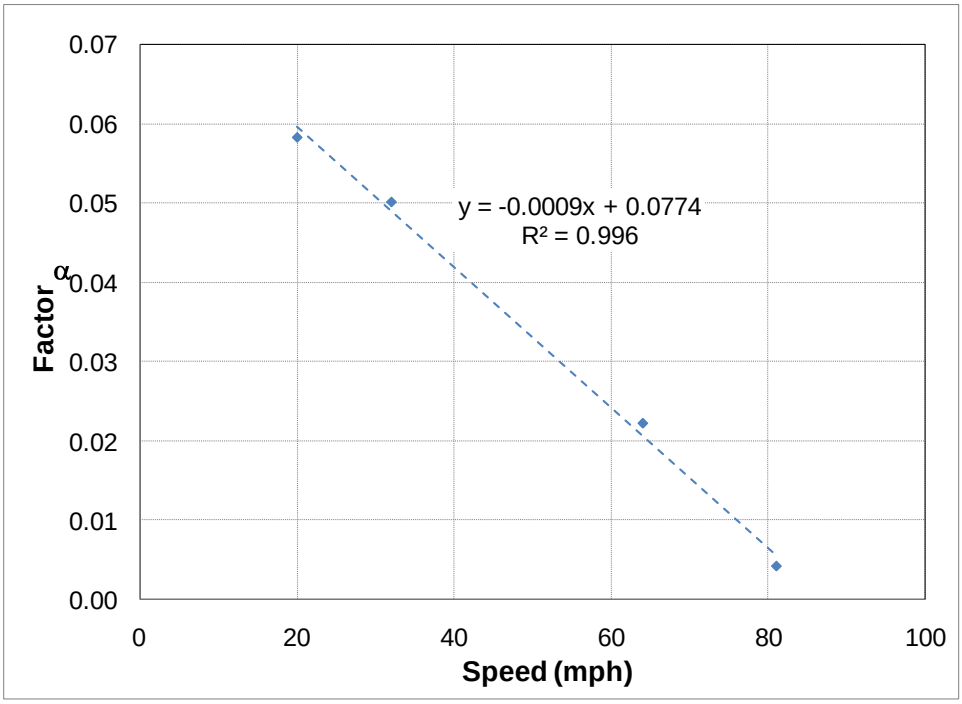

Figure 29. Correlation Between Speed and Factor Alpha (α)

The resulting plots for this model are very similar to the ones obtained without including the speed in Equation 5.1.

5.4 Friction Model for Correction Factors Using the Locked-Wheel Device

The average measured and predicted friction correction factors considering all the dense graded surface mixes for the LWD device is summarized in Table16.

Table 16. Average Monthly Friction Correction Factors for Measurements Taken with the Locked-Wheel Device on the Dense Graded Mixes

Test Date		**Dec**	**Jan**	**Feb**	**Mar**	**Apr**	**May**	**Jun**	**July**	**Aug**	**Sep**
Average Temp (°F)		**39**	**36**	**29**	**48**	**51**	**62**	**69**	**70**	**76**	**67**
32 kph (20mph)	Meas.	1.06	1.02	1.06	1.02	1.05	1.03	1.03	1.05	1.00	1.00
	Model	1.01	1.03	1.03	1.03	1.03	1.02	1.02	1.01	1.00	1.00
64 kph (40mph)	Meas.	1.09	1.05	1.12	1.06	1.05	1.06	1.02	1.08	1.00	1.02
	Model	1.03	1.07	1.08	1.08	1.07	1.05	1.03	1.01	1.00	1.00
80 kph (50mph)	Meas.	0.99	1.01	1.07	1.05	0.99	1.07	0.91	1.00	1.00	1.02
	Model	1.00	1.00	1.00	1.00	1.00	1.00	1.00	1.00	1.00	1.00

Test Date		**Oct**	**Nov**	**Dec**	**Jan**	**Feb**	**Mar**	**April**	**May**	**June**
Average Temp (°F)		**59**	**43**	**39**	**32**	**38**	**44**	**52**	**59**	**70**
32 kph (20mph)	Meas.	1.02	1.02	1.03	0.99	1.02	1.00	1.05		0.99
	Model	1.00	1.01	1.02	1.03	1.03	1.03	1.03	1.02	1.02
64 kph (40mph)	Meas.	0.99	1.03	1.08	1.04	1.06	1.09	1.11		0.99
	Model	1.01	1.03	1.06	1.07	1.08	1.08	1.07	1.05	1.03
80 kph (50mph)	Meas.	0.87	0.89	1.03	0.99	0.98	1.00	1.00		0.92
	Model	1.00	1.00	1.00	1.00	1.00	1.00	1.00	1.00	1.00

A similar analysis was conducted for the measurements with the locked-wheel device. The average measured and predicted monthly friction correction factors at 32, 64, and 80 kph (20, 40, and 50 mph) are presented in Figures 30, 31, and 32, respectively. Figure 30 suggests that the friction correction factors for the measurements at 32 kph (20 mph) using the locked-wheel device do not have a clear cyclical variation. However, it is important to note that this speed is difficult to maintain and additional variations may be introduced because of fluctuations in speed.

At 64 kph (40 mph), which is the standard speed according to ASTM E-274-97, the model fits the data better, showing that friction increases in the winter months and decreases in summer months, as seen in Figure 31. The figure also shows that the lowest friction value occurs in August and the highest in February. The model for 80 kph (50 mph) does not show a good fit for the measurements, and it has a high standard error of 0.058.

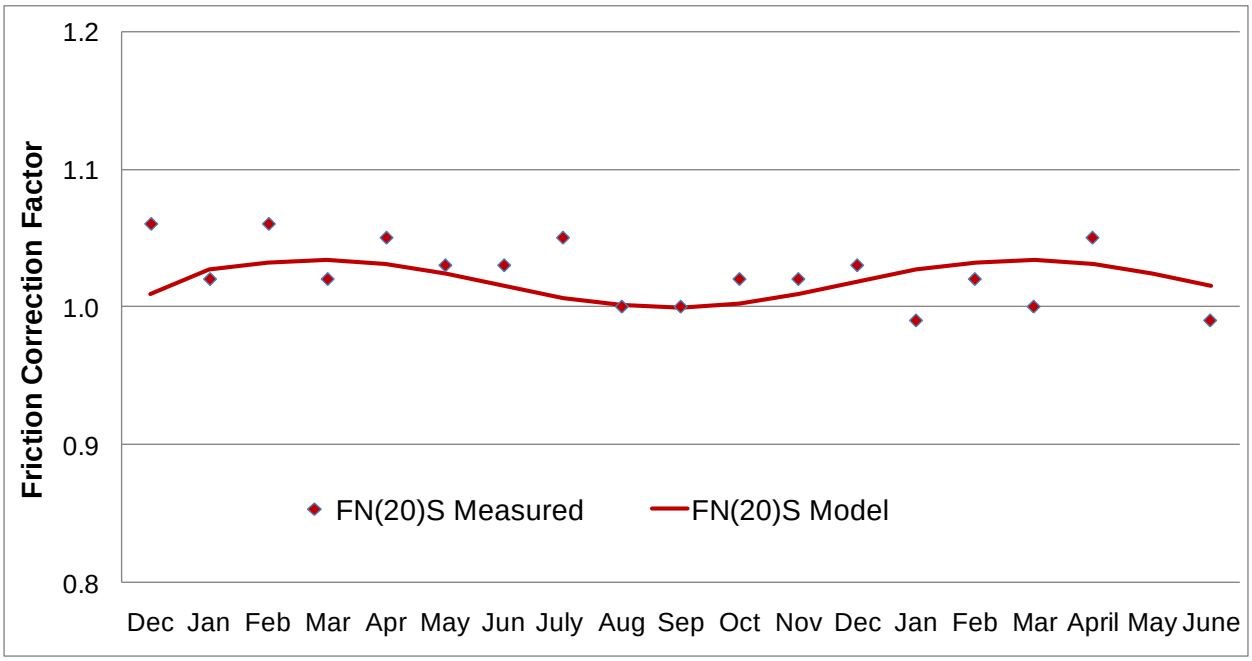

Figure 30. Predicted and Average Measured Friction Correction Factors for the Locked-Wheel Device at 32 kph (20 mph)

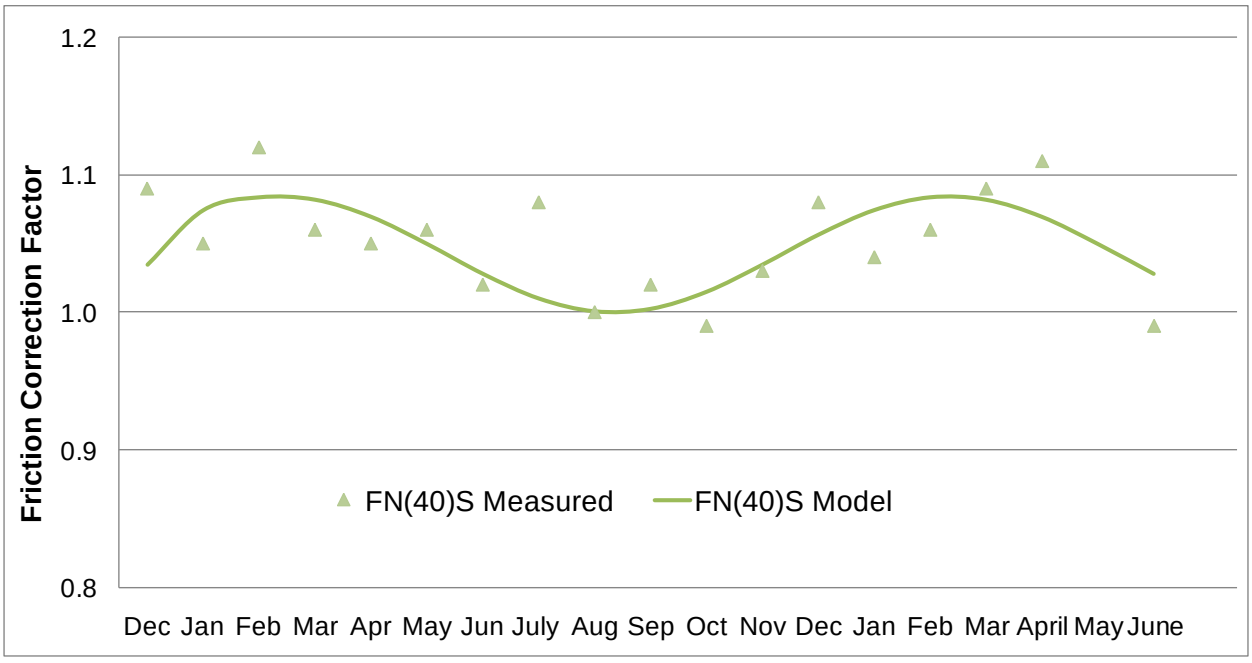

Figure 31. Predicted and Average Measured Friction Correction Factors for the Locked-Wheel Device at 64 kph (40 mph)

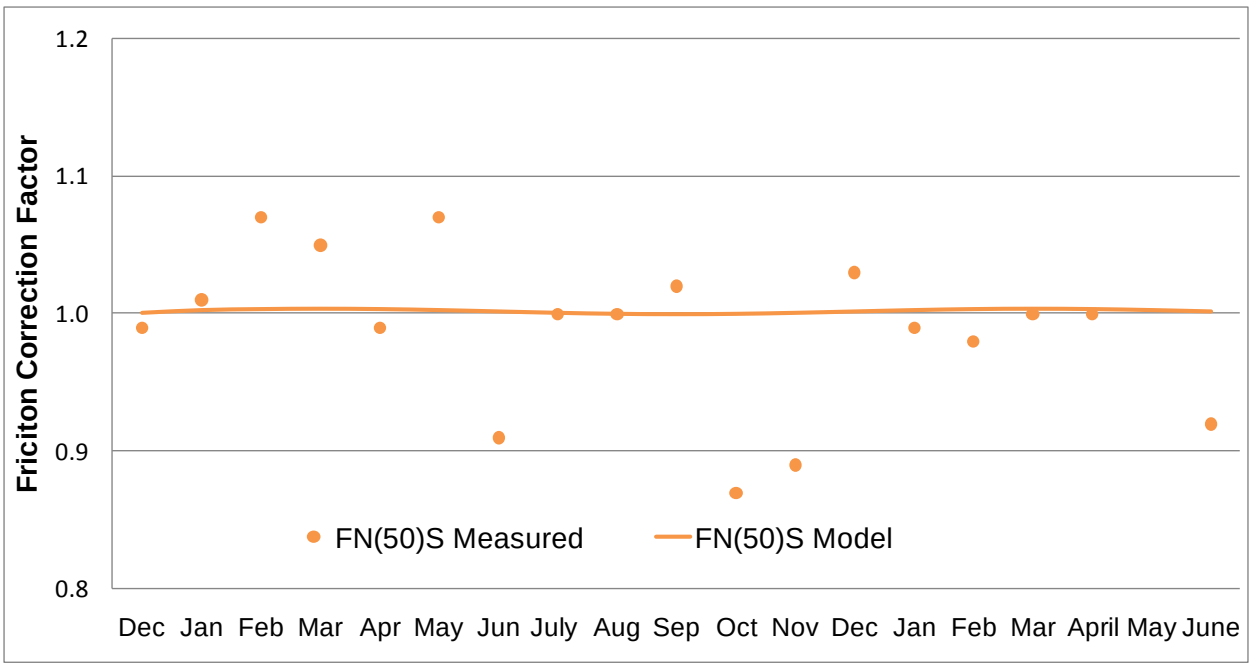

Figure 32. Predicted and Average Measured Friction Correction Factors for the Locked-Wheel Device at 80 kph (50 mph)

Figure 33 shows the average temperatures for the tested months in Blacksburg (NCDC, 2008) and compares them with the fitted sinusoidal model for speeds at 32, 64, and 80 kph (20, 40, and 50 mph). The monthly variation at 64 kph (40 mph) is similar to the one observed with the DFTester correction factors. It suggests that the temperature of the month influences the friction correction values. However, at 32 kph (20 mph) and 64 kph (40 mph) this effect is not clear.

5.5 Effect of Temperature on the Friction Correction Factors

The previous sections suggested that temperature is a factor that contributes to the seasonal friction variation. To investigate this effect, the friction factors obtained for every month at various speeds and with both devices were plotted against the average monthly temperature in Blacksburg (obtained from the National Climatic Data Center).

The friction correction factors for the two friction devices are plotted against the temperature in Figures 34 and 35. In both cases there is a trend in which the correction factors decrease with higher temperatures and speeds, indicating that the effect is less at higher speeds.

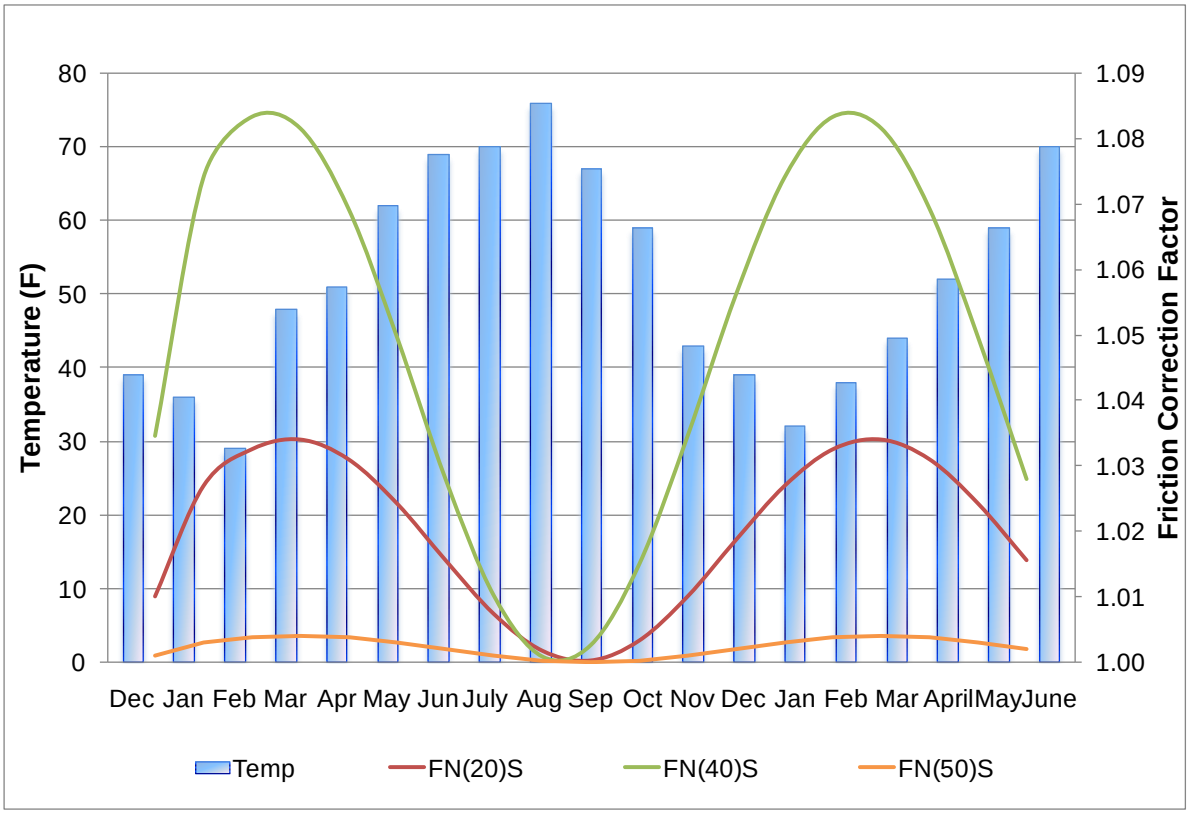

Figure 33. Locked-wheel Device Friction Correction Factors and Average Monthly Temperatures in Blacksburg, December 2006 through June 2008

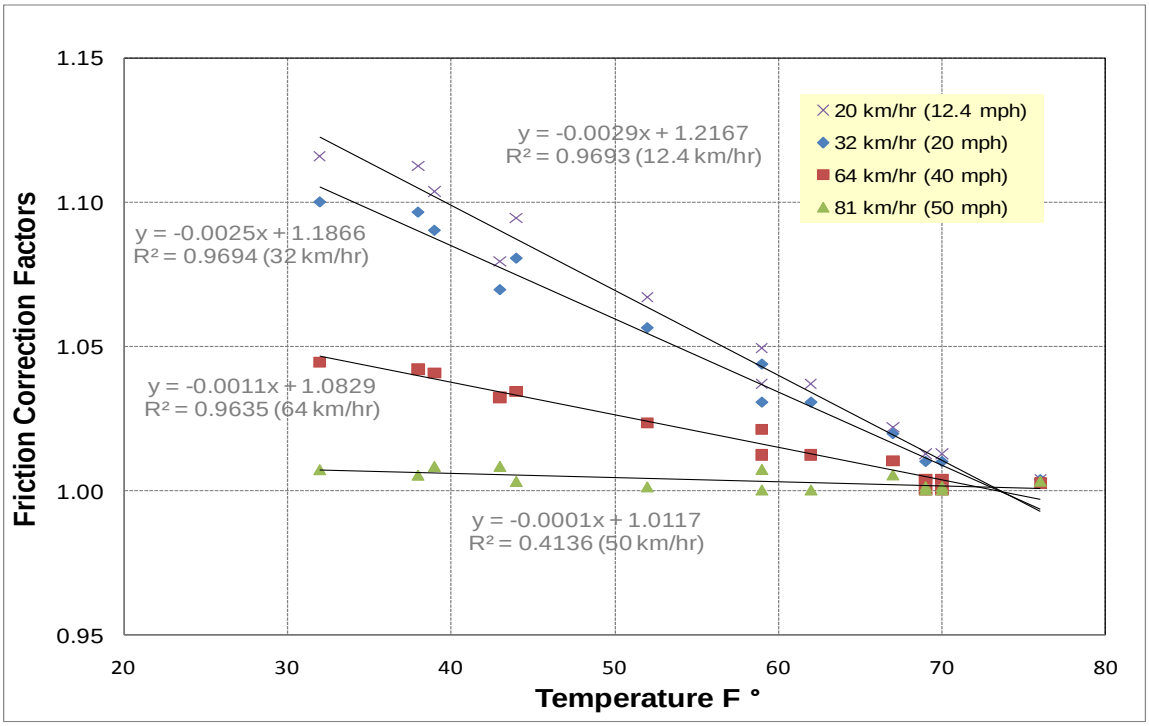

Figure 34. Average Measured Friction Correction Factors for the DFTester vs. Temperature

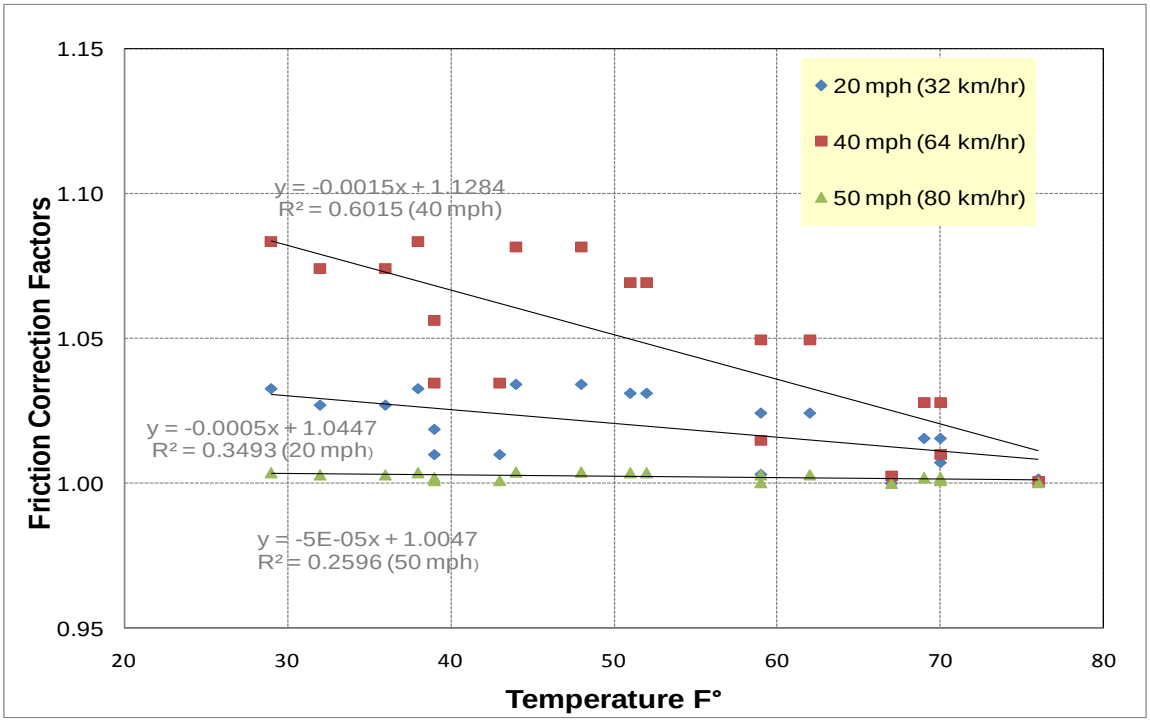

Figure 35. Average Measured Friction Correction Factors for the Locked-wheel Device vs. Temperature

The coefficient of determination (R^2) for the relationships between temperature (in F°) and friction correction factors is higher for the DFTester than for the locked-wheel device. Furthermore, R^2 for the DFTester for all speeds, except 80 kph (50 mph), is above 0.96, which indicates a good relationship between temperature and friction factors. For the locked-wheel device, the highest R^2 occurs at 64 kph (40 mph), which is the model that shows a cyclical season pattern. These results confirm that temperature is one of the main factors that contribute to the seasonal friction variation.

The trend observed in Figures 34 and 35 show that temperature influences friction measurements with both devices. However, the effect is greater using the DFTester than the locked-wheel device. The general trend is that friction values decrease with higher temperatures. For the DFTester friction correction factors, the effect of temperature is higher at lower speeds.

5.6 Model Discussion

The analysis of the collected data and the developed sinusoidal model indicate that there is a significant seasonal variation on the friction measurements taken at different times during the year.

Furthermore at least some of the variation appears to follow a cyclical pattern. Therefore it is logical to assume that this component of the measurement variability occurs in response to some common factors, such as temperature and precipitation. The developed models can be used to predict that trend with a reasonable degree of accuracy for friction correction factors resulting from measurements with the DFTester at 20, 32, and 64 kph (12.4, 20, and 40 mph) and the locked-wheel device at 64 kph (40 mph). On the other hand, the models developed for the locked-wheel device friction correction factors at 32 kph and 80 kph (20 mph and 50 mph) do not fit the measured data very well.

In particular, the model for the measurements at 80 kph (50 mph) cannot model the field data properly. This might be due to fact that friction was more difficult to measure at higher speeds, especially for the locked-wheel device. Since the tested sections are short, the equipment had to be triggered very often, and it was difficult to maintain speed.

Factors other than air temperature and precipitation may explain the rest of the variation. Some of these factors are listed following:

- Differences in water temperature.
- Calibrations of the locked-wheel device occurred in the analysis period.
- Two different locked-wheel trailers were used interchangeably.
- Measurements using the locked-wheel device may have varied throughout sections because this device measures at high speed. For example, it was difficult to conduct all monthly tests on the same paths (lateral test position), and the starting and finishing measurements (longitudinal position) are not always the same. Especially at higher speeds (80 kph [50 mph]), the device might have tested the initial parts of the following section.
- Wear in the rubber pads for the DFTester. Although these pads were replaced on each set of tests, some of the sections were tested with thinner pads than others.

5.7 Effect of Macrotexture on the Friction Correction Factors

It is well known that pavement surface texture affects friction. As discussed in Chapter 2, the two main components of friction are adhesion and hysteresis. Since hysteresis is affected by macrotexture, one should expect that macrotexture would have a significant effect on the dependence of friction measurements on environmental factors. To investigate this hypothesis, the effect of macrotexture on the obtained winter friction correction factors was investigated. The average factors obtained for every section in the months January and February 2008 at various speeds were determined for measurements taken with the locked-wheel device and the DFTester. Table 17 summarizes the average winter friction

correction factors and texture measurements for all the sections investigated. The MPD column shows the average mean profile depths measured for the months of January and February 2008.

Table 17. Average Winter Friction Correction Factors and Macrotexture

Lane	Section	CTMeter MDP	DFTester			Locked-Wheel Device		
			32 kph (20 mph)	64 kph (40 mph)	81 kph (50 mph)	32 kph (20 mph)	64 kph (40 mph)	81 kph (50 mph)
EASTBOUND	Loop average	1.04	1.08	1.04	1.01	1.00	1.10	1.07
	A average	0.57	1.13	1.09	1.04	1.08	1.06	0.94
	B average	0.73	1.11	1.06	1.02	1.03	1.10	0.94
	C average	0.68	1.11	1.05	1.02	1.06	1.10	1.03
	D average	0.56	1.09	1.02	1.00	1.14	1.26	1.05
	I average	0.85	1.08	1.03	1.01	1.04	1.11	0.99
	J average	0.92	1.11	1.06	1.03	0.98	1.01	0.99
	K average	1.51	1.08	1.04	1.01	0.90	0.85	0.91
	L average	0.93	1.05	0.99	0.96	0.98	1.02	0.98
WESTBOUND	L average	1.06	1.09	1.03	1.02	0.97	1.01	1.02
	K average	1.65	1.05	1.01	0.98	0.92	0.88	0.88
	J average	0.84	1.11	1.05	1.03	1.02	0.99	0.94
	I average	0.71	1.09	1.04	1.03	1.02	1.00	1.10
	D average	0.68	1.11	1.05	1.02	1.06	1.04	1.05
	C average	0.74	1.10	1.05	1.02	1.01	1.00	1.00
	B average	0.99	1.06	1.03	0.92	0.99	1.06	0.98
	A average	0.83	1.06	1.03	0.92	1.01	1.06	1.03
	Loop average	0.88	1.11	1.06	0.89	0.95	1.17	1.13
Overall	*Average*	*0.90*	*1.09*	*1.04*	*1.00*	*1.01*	*1.05*	*1.00*

The winter monthly friction correction factors for the two friction devices studied are plotted against the macrotexture in Figures 36 and 37. In both cases there is a trend of the correction factors decreasing with increasing macrotexture, indicating that the effect of seasonal factors on the friction measurements is less on those sections with greater macrotexture. The coefficient of determination for the relationships between macrotexture and friction correction factors (R^2) is higher for the locked-wheel device than that obtained with the DFTester. However, R^2 are highest at 32 kph (20 mph) using the DFTester, and at 64 kph (40 mph) using the locked-wheel device.

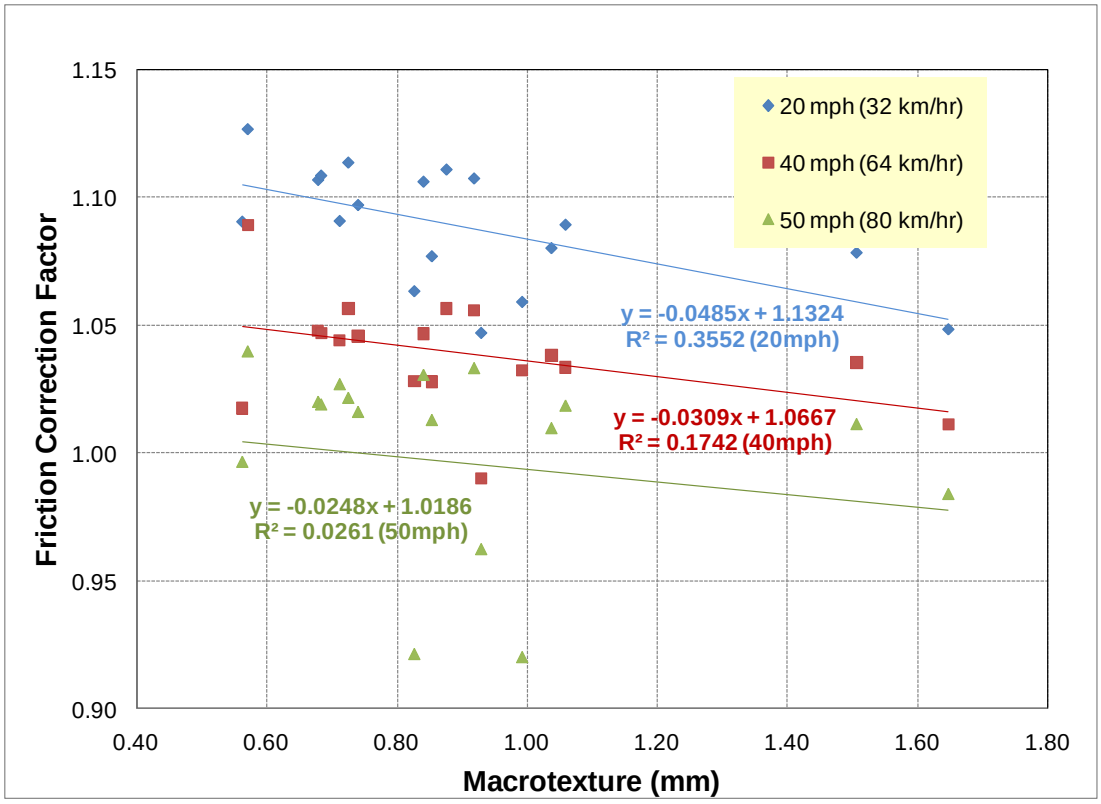

Figure 36. DFTester Friction Factors versus Macrotexture

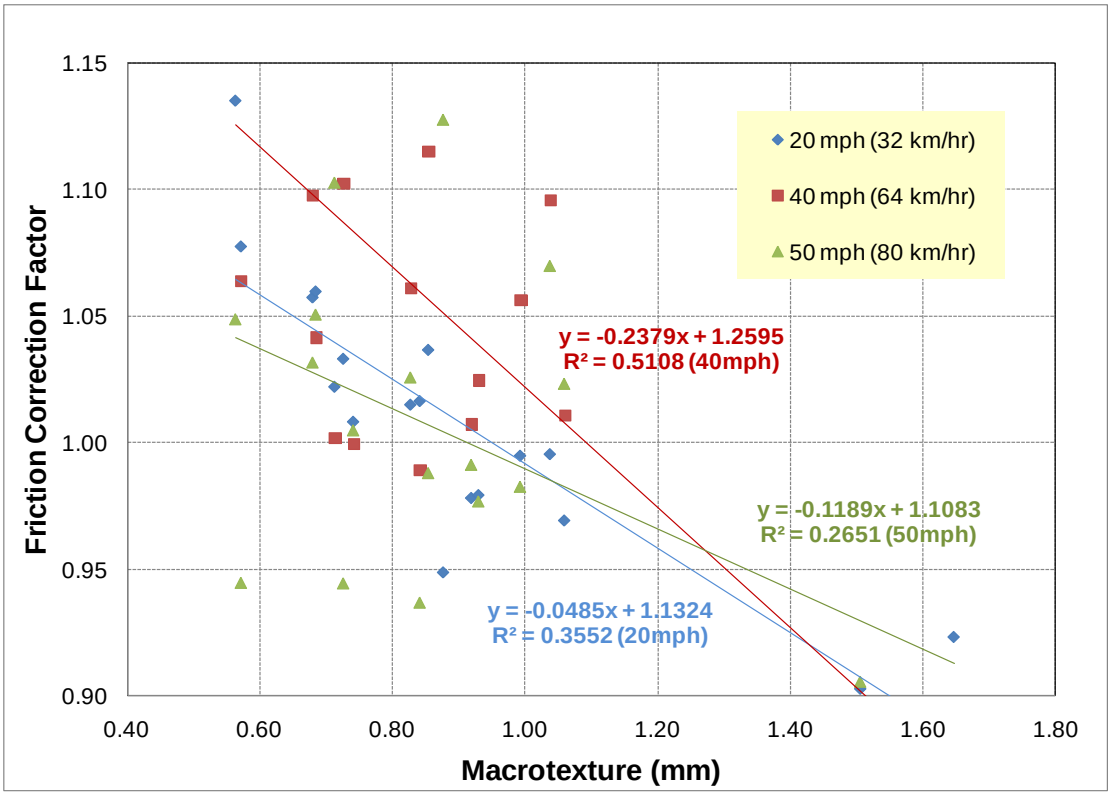

Figure 37. Locked-Wheel Device Friction Correction Factors versus Macrotexture

The trend observed in Figures 36 and 37 suggests that macrotexture influences the impact of seasonal factors on friction measurements with both devices. However, the influence of macrotexture is greater using the locked-wheel device than the DFTester. For the DFTester friction correction factors, the effect of macrotexture seems to decrease at higher speeds. This effect is not evident on the locked-wheel friction correction factors.

5.8 Summary

This chapter analyzed the effect of seasonal variation on pavement friction properties and the impact of macrotexture on the correction factors. Friction values were normalized by dividing the value obtained each month by the August 2007 values. The resulting numbers were considered friction correction factors that can be use to bring the measurements to their lowest value. Sinusoidal models were fitted to data to predict monthly correction factors for different speeds using both devices. Models for DFTester correction factors at 20, 32, and 64 kph (12.4, 20, and 40 mph), and for the locked wheel at 64 kph (40 mph) show a cyclical tendency: friction measurements are higher in the winter than in the summer. The lowest correction factor occurs in the hottest months of the year. It was also observed that the temperature of the month and the speed of the test are two of the main factors influencing the friction correction factors. The impact of temperature on the DFTester friction correction factors obtained with the fitted model is high for measurements at 20, 32, and 64 kph (12.4, 20, and 40 mph). It was also observed that the influence of temperature on these values decreases with speed.

The effect of macrotexture on the average friction correction factors obtained for every section in the months January and February 2008 shows that the required correction decrease with increased macrotexture. This effect is observed for both devices. However, the coefficient of determination for the relationships between macrotexture and friction correction factors (R^2) is greater for the locked-wheel device than for that obtained with the DFTester. The lowest coefficient of determination occurs for both devices at 80 kph (50 mph).

CHAPTER 6. FINDINGS AND CONCLUSIONS

Pavement friction properties are affected by environmental factors, such as temperature, contaminants, rainfall, and dry days before the test. Although the effects of these factors have been studied by several researchers around the world, the seasonal variations are still not well understood. This thesis investigated seasonal environmental effects on friction surface properties. In order to accomplish this, friction tests were conducted monthly using two locked-wheel devices and a DFTester on nine asphalt pavement sections at the Virginia Smart Road. Due to the low traffic in the facility and the time period of this investigation, only seasonal changes were considered.

6.1 Findings

The analysis of the monthly data collected on the Smart Road led to the following findings:

- Friction measurements on the evaluated pavement sections experienced significant variations throughout the year. The general trend is that higher friction values were measured in the winter than in the summer.

- Furthermore, the average friction seasonal variations follow a cyclical pattern. The average friction measurements with the locked-wheel device and the DFTester were found to follow an approximately sinusoidal pattern.

- Sinusoidal models were found appropriate to predict the correction factors necessary to adjust friction measurements obtained throughout the year. The resulting models fit the average friction measurements obtained with the DFTester better than those measured with the locked-wheel device.

- The correction factors follow a similar pattern as the temperature variations. This suggests that temperature was at least one of the factors that affected the fiction correction factors. In this case, again, the coefficients of determination for the temperature-friction correction factors relationship were higher for the DFTester than those obtained for the measurements with the locked-wheel device.

- The slip speed at which friction is measured and/or recorded is another factor that should be considered. The magnitude of the required correction factors for the DFTester measurements decrease with higher speeds. At 80 kph (50 mph) the measurements do not appear to be influenced by the seasonal changes.

- The macrotexture of the pavement surface appears to have an effect on the magnitude of the correction. The maximum (winter) friction correction factors were found to decrease with increased macrotexture for both devices at all speeds. The effect is more pronounced for the locked-wheel measurements than for the DFTester measurements.

- It was observed that the friction measurements on section K, the OGFC, followed a different behavior throughout the year. However, there was not enough data to draw strong conclusions about the specific trend for these types of mixes.

- The developed models fit the average friction measurements better at 20 kph, using the DFTester, and at 40 mph using the locked-wheel trailer. These two speeds are the standard speeds for these devices according to the ASTM.

6.2 Conclusions

The main conclusion of this investigation is that seasonal variation has a significant effect on pavement friction measurements. The general trend observed is that the measurements are higher in the winter months than in the summer months. This tendency follows a cyclical sinusoidal pattern throughout the year.

Sinusoidal models can be used to predict the seasonal changes of friction throughout the year. Better coefficients of determination were obtained for the DFTester than for the locked-wheel device. However, for the locked-wheel device at 64 kph (40 mph), which is the standard speed of the test according to the ASTM E-274-97, the sinusoidal model determined fit relatively well the measured friction correction factors. Average friction correction factors for the Commonwealth of Virginia were proposed using these models.

6.3 Recommendations

Although it was found that seasonal variation has a significant effect on pavement surface friction and that correction factors may correct this effect, it is recommended that more studies be conducted to fully understand the magnitude of these variations. The following additional studies are recommended for this purpose:

- Study the effect in different weather locations. Temperature variations may affect the results of the investigation, thus correction factors should not be the same.
- Consider the number of dry days before the test as an additional variable. Dust and contaminant

accumulation may also affect the measured friction.

- Conduct additional tests to study the effect of the temperature of the water, dry pavement, and wetted pavement, as well as tire temperature on the friction measurements.
- Investigate the effect of wear of the DFTester's sliders on the friction measurements. The friction measurements obtained at selected locations with new pads were consistently higher than those with used ones.

REFERENCES

AASHTO, American Association of State Highway and Transportation Officials. 1996. "Standard Method of Test for Frictional Properties of Paved Surfaces Using a Full-Scale Tire". *AASHTO T242*.

ASTM, American Society for Testing Materials. 2000. "Standard Definition of Skid Resistance". *ASTM E-17*.

ASTM, American Society for Testing and Materials, Anderson, D. A., Meyer, W. E., and Rosenberger, J. L. 2000. "Standard Smooth Tire for Pavement Skid-Resistance Tests." *ASTM E-524, Annual Book of ASTM Standards.* Vol. 4.03.

ASTM, American Society for Testing and Materials. 2000. "Standard Rib Tire for Pavement Skid-Resistance Tests." *ASTM E-501, Annual Book of ASTM Standards.* Vol. 4.03.

ASTM, American Society for Testing and Materials. 2000. "Skid Resistance of Pavements Using a Full-Scale Tire." *ASTM E-274-97 Annual Book of ASTM Standards.* Vol. 4.03.

ASTM, American Society for Testing and Materials. 2000. Standard Test Method for Measuring Paved Surface Frictional Properties Using the Dynamic Friction Tester. *ASTM E-1969*.

ASTM, American Society for Testing and Materials. 2000. Standard Practice for Calculating International Friction Index of a Pavement Surface. *ASTM E-1960 -07*.

ASTM, American Society for Testing and Materials. 2000. Standard Test Method for Measuring Paved Surface Frictional Properties Using the Dynamic Friction Tester. *ASTM E-1911-98.*

ASTM, American Society for Testing and Materials. 2000. Practice for Calculating Pavement Macrotexture Mean Profile Depth. *ASTM E-1845*.

ASTM, American Society for Testing and Materials. 2000. Standard Test Method for Measuring Pavement Macro-texture Properties Using the Circular Track Meter. *ASTM E-2157.*

Anderson, D., Meyer, W., and Rosenberger, J. 1984. "Development of a Procedure for Correcting Skid-Resistance Measurements to a Standard End of Season Value." *Transportation Research Record* No. 1084:40-48.

AUSTROADS. 2004. "Guidelines In the Management Of Road Surface Skid Resistance." *Project No. BS.A.N. 553*.

Bazlamit, S., and Reza, F. 2005. "Changes in Asphalt Friction Components and Adjustment Number for Temperature." *The Journal of Transportation Engineering,* ASCE 2005:131-470.

Burchett, J., and Rizenbergs, R. 1980. "Seasonal Variations in the Skid Resistance of Pavements in Kentucky." Transportation Research Record, No 788: 12.

Caltrans, Division of Maintenance. 2007. "Chapter 2 Surface Characteristics". *MTAG, Rigid Pavement Preservation.* Volume II, second Edition:2-20.

Cenek, P., Alabaster, J., and Davies, B. 1999. "Seasonal and Wheater Normalisation of Skid Resistance Measurement." *Transfund Research Report* 139.

Colony, D. 1992. "Influence of traffic, surface age and environment on skid number" *Ohio Department of Transportation Project Number 14460* Final Report, Columbus, Ohio.

Croney, D., and Croney, P. 1998. "Design and performance of road pavements". *McGraw Hill, New York*, 3rd Edtion: 471-472.

Dahir, H., and Henry, J. 1979. "Final Report: Seasonal Skid Resistance Variations." Pennsylvania Department of Transportation. *Transportation Research Board* 715.

de Solminihac, C., and Echaveguren, T. 2007. "Procedure to Process, Harmonize and Analyze Grip Tester Measurements." *Pontificia Universidad Catolica de Chile, Departamento de Ingenieria y Gestion de la Construccion*.

Donbavand, J., and Cook, D. 2004. "Procedures for correcting Seasonal Variation." *Transit New Zealand* (Correcting Seasonal Variations): 2-3.

Elkin, L., Kercher, J., and Gulen, S. 1980. "Seasonal Variation in Skid Resistance of Bituminous Surfaces in Indiana." *Transportation Research Record* No 777:50-58.

Faung, H., and Hughes, W. 2007. "Friction Monitoring of SuperPave Mixes in Virginia." *Virginia Highway & Transportation Research Council*: 8-9.

Flintsch, G., de Leon, E., McGhee, K., and Al-Quadi, L. 2003. "Pavement Surface Macrotexture Measurements and Application." *Transportation Research Board*, Journal of the Transportation Research Board, No 1860, Washington, D.C. (Paper # 03-3436):38-43.

Giles, C., Sabey, E., and Cardew, F. 1964. "Development and Performance of the Portable skid resistance tester." *Road Research Technical Paper Number 66*, London.

Hall, L., Titus-Glover, L., Smith, D., and Evans, D. 2006. "Guide for Pavement Friction, Final Guide." *Transportation Research Board*, NCHRP 1-43, Transportation Sector of Applied Researcher Associates (ARA): 39-59.

Hill, J., and Henry, J., 1978. "Short Term, Weather-Related Skid Resistance Variation." Transportation Research Record, No. 836:76-81.

Henry, J. 1983. "Comparison of Friction Performance of a Passenger Tire and the ASTM Standard Test Tires." *ASTM STP 793* ASTM (Philadelphia, Pennsylvania).

Henry, J. 2000. "Evaluation of Pavement Friction Characteristics, A Synthesis of Highway Practice." *NCHRP Synthesis 291*, Transportation Research Board, Washington D.C.

Hill, J., and Henry, J. 1982. "Mechanistic Model for Predicting Seasonal Variations in Skid Resistance." *Transportation Research Board* No 946:29-37.

Jayawickrama, P., and Thomas, B. 1998. "Correction of Field Skid Measurements for Seasonal Variations in Texas." *Transportation Research Board* 1639:147-152.

Kennedy, K., Young, E., and Butler, C. 1990. "Measurement of Skidding Resistance and Surface Texture and the Use of Results in the United Kingdom." *Proceedings of a Symposium on Surface Characteristics of Roadways* ASTM 87-101.

Kummer, W., and Meyer, E. 1962. "Measurement of Skid Resistance, Symposium on Skid Resistance." *ASTM Special Technical Publication*, No. 326:3-28.

Leu, C., and Henry, J. 1976. "Prediction of Skid Resistance as a Function of Speed from Pavement Texture." *Transportation Research Record, TRB, National Research Council.* No.946.

Li, S., Noureldin, S., and Zhu, K. 2004. "Upgrading the INDOT Pavement Friction Testing Program." *Joint Transportation Research Program,* Perdue Libraries: 6-9.

Luo, Y., Flintsch, G., and Al-Quadi, L. 2004. "Analysis of the Effect of Pavement Temperature on the Frictional Properties of Flexible Pavements Surface." *Transportation Reseach Board* 2005, TRB Annual Meeting of the Transportation Research Board.

Maryland State Highway Administration, Office of Traffic and Safety, Traffic Safety Analysis Division. 2002. "State System (MD,US,IS) Roads Accident and Wet Surface Accident Profile Sheet Accident Information."

Meyer, H., and Kummer, E. 1967. "Tentative Skid-Resistance Requirements for Main Rural Highways." *National Cooperative Highway Research Program NCHRP Washington, D.C.* No 37.

Mitchell, J., Phillips, M., and Shah, G. 1986. "Report No. FHWA/MD-86/02: Seasonal Variation of Friction Numbers." *Maryland Department of Transportation (MDOT)* Baltimore.

National Climatic Data Center. 2008. "Climatic of 2008 Annual Review: Month-by-Month Variability in U.S." *Asheville, N.C.*

NHCRP. 1992. "Estimation of Skid Numbers from Surface Texture Parameters in the Rational Design of Standard Reference Pavements for Test Equipment Calibration." *Journal of Testing and Evaluation, JTEVA, Vol 2. March 1974,* March 1974:73-83.

NHCRP. 2000. "Evaluation of Pavement Friction Characteristics." *A synthesis of Highway Practice.* Synthesis 291*:57.*

National Highway Traffic Safety Administration (NHTSA). 2004. "Traffic Safety Facts." *NHTSA,* 400. Washington, D.C. 6-8.

Noyce, D., and Bahia, H. 2005. "Incorporating Road Safety Into Pavement Management: Maximizing Surface Friction for Road Safety Improvements." *Technical Report University of Wisconisn, Madison.*

Oliver, J., 1980. "Temperature Correction of Skid Resistance Values Obtained with the British Pendulum Skid Resistance Tester." *Australia Road Research Board* Internal Report AIR 314-2.

Oliver, J., Tredrea, P., and Pratt, D. 1988. "Seasonal Variation of Skid Resistance in Australia." *Australia Road Research Board* Special Report No. 37:1-17.

Runkle, D., and Mahone, S. 1980. "Variation in Skid Resistance Over Time." *Virginia Highway & Transportation Research Council*: 10-13.

Tung, J., Henry, J., and Dahir, S. 1977. "Statistical Analysis of Seasonal Variations in Pavement Skid Resistance." The Pennsylvania Transportation Institute, Department of Transportation Bureau of Materials, Testing and Research, Research Report: 75-90.

Wambold, J., and Andresen, C. 1999. "Friction Fundamentals, Concepts and Methodology." *Transportation Development Centre Transport Canada* TP 13837E:68-70.

Wambold, J., and Henry, J. 1996. "Use of Smooth-Treated Tire in Evaluating Skid Resistance." *Transportation Research Record* No. 1348: 35-41.

Wilson, D., 2006. "An Analysis of the Seasonal and Short-Term Variation of Road Pavement Skid Resistance." *Thesis submitted for the degree of Philosophy in Engineering, the University of Auckland*.